



Office of
Environment
& Heritage



Lower Hunter Particle Characterisation Study

Supplementary Report – Chemical Transport Modelling Case Studies

Kathryn M. Emmerson (CSIRO), Martin E. Cope (CSIRO), Mark F. Hibberd (CSIRO), Paul W. Selleck (CSIRO), Marcus Thatcher (CSIRO) and Yvonne Scorgie (OEH)

Final report to the NSW Environment Protection Authority

April 2016

The NSW Environment Protection Authority (NSW EPA) commissioned this report from the Office of Environment and Heritage (OEH) and CSIRO.

This report was prepared by OEH and CSIRO in good faith exercising all due care and attention, but no representation or warranty, express or implied, is made as to the relevance, accuracy, completeness or fitness for purpose of this document in respect of any particular user's circumstances. Users of this document should satisfy themselves concerning its application to, and where necessary seek expert advice in respect of, their situation. The views expressed within are not necessarily the views of the NSW EPA and may not represent NSW EPA policy.

Citation:

Emmerson, KM, Cope, ME, Hibberd, MF, Selleck, PW, Thatcher, M and Scorgie, Y. (2016). Lower Hunter Particle Characterisation Study Supplementary Report – Chemical Transport Modelling Case Studies. Report prepared by CSIRO and the NSW Office of Environment and Heritage on behalf of the NSW Environment Protection Authority, April 2016.

Cover photograph: courtesy of the Hunter Development Corporation

© 2016 CSIRO, State of NSW and OEH

With the exception of photographs, the State of NSW, OEH and CSIRO are pleased to allow this material to be reproduced in whole or in part for educational and non-commercial use, provided the meaning is unchanged and its source, publisher and authorship are acknowledged. Specific permission is required for the reproduction of photographs.

CSIRO advises that the information contained in this publication comprises general statements based on scientific research. The reader is advised and needs to be aware that such information may be incomplete or unable to be used in any specific situation. No reliance or actions must therefore be made on that information without seeking prior expert professional, scientific and technical advice. To the extent permitted by law, CSIRO (including its employees and consultants) excludes all liability to any person for any consequences, including but not limited to all losses, damages, costs, expenses and any other compensation, arising directly or indirectly from using this publication (in part or in whole) and any information or material contained in it.

OEH has compiled this technical report in good faith, exercising all due care and attention. No representation is made about the accuracy, completeness or suitability of the information in this publication for any particular purpose. OEH shall not be liable for any damage which may occur to any person or organisation taking action or not on the basis of this publication. Readers should seek appropriate advice when applying the information to their specific needs.

Published by:

Office of Environment and Heritage NSW on behalf of OEH and CSIRO
59 Goulburn Street, Sydney NSW 2000
PO Box A290, Sydney South NSW 1232; Phone: (02) 9995 5000 (switchboard)
Phone: 131 555 (environment information and publications requests)
Phone: 1300 361 967 (national parks, climate change and energy efficiency information, and publications requests); Fax: (02) 9995 5999; TTY: (02) 9211 4723
Email: info@environment.nsw.gov.au; Website: www.environment.nsw.gov.au

ISBN: 978 1 76039 342 7
OEH 2016/0244
April 2016

Contents

Acknowledgments	v
Executive summary	vi
1 Introduction	1
2 The CSIRO modelling framework	2
2.1 Overview.....	2
2.2 Meteorological module.....	3
2.3 Emissions module.....	9
2.4 Chemical transport modelling.....	11
3 Results	12
3.1 Total PM _{2.5}	12
3.2 PM _{2.5} components.....	14
3.3 Spatial variations	18
3.4 Sources of the PM _{2.5} components.....	22
4 Summary	28
References	29

Figures

Figure 1. Flow chart summarising CSIRO modelling framework. Note: VOC – volatile organic carbon; bVOC – biogenic component of the same; EC – elemental carbon; OC – organic carbon; NO _x – oxides of nitrogen; NH ₃ – ammonia; SO ₄ – sulfate.....	2
Figure 2. Map showing positions of the 9 km, 3 km and 1 km modelling grids.....	3
Figure 3 Comparison of measured temperature, wind speed and wind direction at Stockton with model output from CCAM and the UM.	5
Figure 4 Wind roses for Newcastle, Stockton and Beresfield for 1–15 July 2014. Observed data is on the left, modelled predictions from CCAM are on the right.....	6
Figure 5 Wind roses for Newcastle, Stockton, Mayfield and Beresfield for 10–22 November 2014. Observed data is on the left, modelled predictions from the UM are on the right.	7
Figure 6. Emissions of SO ₂ , NH ₃ , organic carbon and levoglucosan for July from the 2008 GMR inventory. Note that maximum emission values for individual point sources greatly exceed the maximum values on the colour legends; the scale was selected to highlight the regional distribution of sources.	10
Figure 7 Modelled and observed 24 hour averaged PM _{2.5} at each of the LHPCS sites for July 2014. The filter samples were only collected every third day.	12
Figure 8 Modelled and observed 24-hour averaged PM _{2.5} at each of the sites for November 2014. The filter samples were only collected every third day.	14
Figure 9 Modelled concentrations of smoke and the secondary organic aerosol produced from the smoke emissions on the Australia-wide grid from CTM using CCAM meteorology.....	14
Figure 10 Comparison of measured and modelled component concentrations of PM _{2.5} for July and November 2014 at Newcastle, Stockton, Mayfield and Beresfield monitoring sites. Note that sum of components here do not equal total PM _{2.5} . Figure continues on next page.	16
Figure 11 Spatial contour plots for modelled total PM _{2.5} and levoglucosan during (left) 1–15 July 2014 and (right) 10– 22 November 2014.....	19
Figure 12 Spatial contour plots for modelled elemental carbon and organic matter during (left) 1–15 July 2014 and (right) 10– 22 November 2014.	20
Figure 13 Spatial contour plots for modelled sea salt and nitrate aerosol during (left) 1–15 July 2014 and (right) 10–22 November 2014.....	21
Figure 14 Spatial contour plots for modelled ammonium and sulfate aerosol during (left) 1–15 July 2014 and (right) 10– 22 November 2014.....	22
Figure 15. Spatial concentration and polar bivariate plots for modelled sea salt for July (left column) and November (right column).....	24
Figure 16. Spatial concentration and polar bivariate plots for modelled elemental carbon for July (left column) and November (right column).	25
Figure 17 Spatial concentration and polar bivariate plots for modelled levoglucosan for July (left column) and November (right column).	26
Figure 18 Modelled component concentrations of PM _{2.5} for July and November 2014 at Maitland and Toronto. Note that sum of components here do not equal total PM _{2.5}	27

Tables

Table 1 Metrics for temperature and wind components at the LHPCS sites. Measurements are compared to CCAM for 1–15 July and compared with the UM for 10–22 November 2014. MB – mean bias; MAGE – mean absolute gross error.....	8
Table 2 List of source categories in the 2008 Sydney GMR inventory	9

Acknowledgments

This project was funded by

- NSW Environment Protection Authority (EPA)
- NSW Office of Environment & Heritage (OEH)
- NSW Ministry of Health
- CSIRO Oceans & Atmosphere (O&A)
- ANSTO

The project was supported by the Project Management Team of Matt Riley (OEH), Yvonne Scorgie (OEH), Judy Greenwood (EPA), Ann Louise Crotty (EPA), Leanne Graham (EPA), Wayne Smith (NSW Health), John Kirkwood (OEH), Keith Craig (NCCCE), Mark Hibberd (CSIRO), Melita Keywood (CSIRO), David Cohen (ANSTO) and Ed Stelcer (ANSTO).

Anthropogenic emissions for the modelling study were largely sourced from the NSW EPA's Greater Metropolitan Region (GMR) Emissions Inventory. Assistance from the NSW Office of Environment and Heritage comprising preparation of GMR emissions data for modelling, supply of air quality and meteorological monitoring data for model evaluation purposes, and provision of advice for the modelling study, is acknowledged.

Executive summary

Chemical transport modelling (CTM) was undertaken for the Lower Hunter Particle Characterisation Study (LHPCS). This modelling report is designed to accompany the main report for the study (Hibberd et al., 2016), which reported the measured particulate components of aerosol in the Lower Hunter valley for one year between March 2014 and February 2015. The modelling concentrates on predicting aerosol components at the fine particulate PM_{2.5} size fraction for July and November 2014 case-study periods. These periods encompass the high wood smoke found in the measurements during winter and the high sea salt measured in late spring/summer. Predicted PM_{2.5} component concentrations are compared to the measurements made at the four LHPCS sampling sites; Newcastle, Stockton, Mayfield and Beresfield.

The model generally predicted the measured aerosol components in the PM_{2.5} size fraction reasonably well for the July 2014 case-study period, but was unable to replicate high ammonium nitrate aerosol concentrations measured at the Stockton site. The under-prediction of ammonium nitrate at Stockton is due to a local source of direct ammonium nitrate emissions not represented in the emission inventory used for the modelling. This source is discussed in more detail in the main report (Hibberd et al., 2016). Furthermore, Eulerian models such as the CTM are unable to predict in-plume concentrations for plumes narrower than the inner grid cell resolution (1 km in this study).

The dominant wind direction in the summer months is onshore, bringing sea salt inland. The model predicted the sea salt components well in November, as well as capturing the sulfate and nitrate aerosol. Organic matter is over-predicted due to long range transport of bushfire smoke from north-west Australia, which has undergone fast chemical processing to form secondary organic aerosol under the higher peak temperatures predicted by the meteorological model, CCAM.

The modelled spatial distributions showed that the four study sites generally predicted the range of modelled PM_{2.5} and PM_{2.5} component concentrations well, except for some localised sources of elemental carbon and organic matter. The model results demonstrate the importance of the continental scale transport of sea salt in determining inland background concentrations in winter.

The measured PM_{2.5} component information from the LHPCS is very useful for the purpose of refining and validating chemical transport modelling for the region. This modelling in turn has enabled the projection of spatial trends in PM_{2.5} component concentrations across the Lower Hunter region, and the projection of PM_{2.5} component concentrations at sites for which measurements were not undertaken, as illustrated in this report for Maitland and Toronto.

1 Introduction

The Lower Hunter Particle Characterisation Study provides details on the components and sources of fine ($PM_{2.5}$) and coarse ($PM_{2.5-10}$) air particles in the Lower Hunter region based on sampling and analysis at four locations over the period March 2014 to February 2015 (Hibberd et al., 2016).

Chemical transport modelling was undertaken for two case-study periods during the Lower Hunter Particle Characterisation Study, with winter (1–15 July 2014) and spring (10–24 November 2014) periods selected to further investigate seasonal differences in $PM_{2.5}$ component concentrations.

The aims of the modelling were:

- (i) to assess model performance against observed meteorology and measured components of the fine particle aerosol;
- (ii) to model the spatial variability of the $PM_{2.5}$ component concentrations to extend the knowledge gained in the measurements program at four specific sites to the wider Lower Hunter region; and
- (iii) to assist in determining the sources and mechanisms responsible for the generation of $PM_{2.5}$.

This modelling report is designed to accompany Hibberd et al. (2016), which reported the measured particulate components of aerosol in the Lower Hunter valley for one year between March 2014 and February 2015. This report focuses on modelling the aerosol components of the fine particulate ($PM_{2.5}$) size fraction.

2 The CSIRO modelling framework

2.1 Overview

The CSIRO model is considered as a framework, combining modules of meteorology, emissions and chemical and physical processes. A flow chart of the modelling framework is shown in Figure 1.

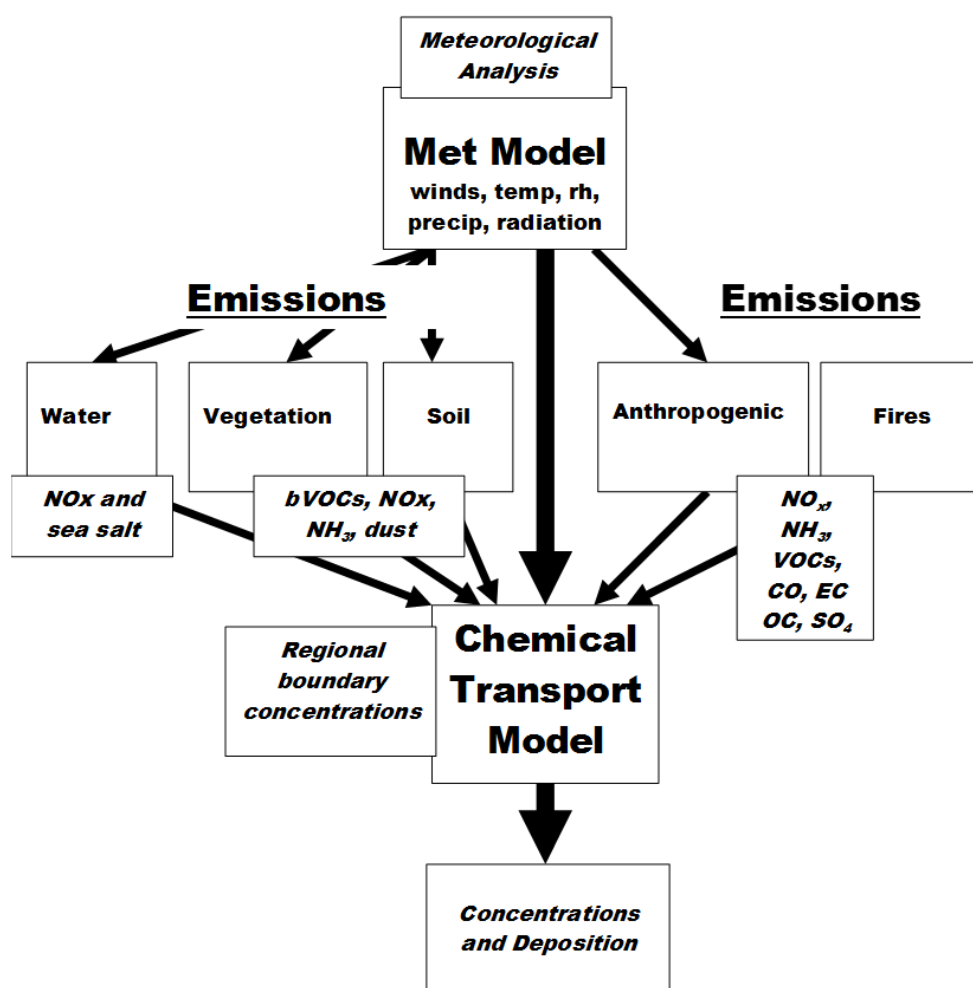


Figure 1. Flow chart summarising CSIRO modelling framework. Note: VOC – volatile organic carbon; bVOC – biogenic component of the same; EC – elemental carbon; OC – organic carbon; NO_x – oxides of nitrogen; NH₃ – ammonia; SO₄ – sulfate.

The model domains that have been chosen for the Lower Hunter study include both the larger scale continental processes and the finer resolution processes occurring within the valley itself. A five-grid system is used for this purpose, using an 80-km grid resolution for the Australia-wide domain nesting down to 1-km grid resolution within the valley. Each outer grid then provides the boundary conditions to each successively

finer grid. A 27-km resolution grid is used to cover South East Australia. It houses grid resolutions at 9 km, 3 km and 1 km as shown in Figure 2.

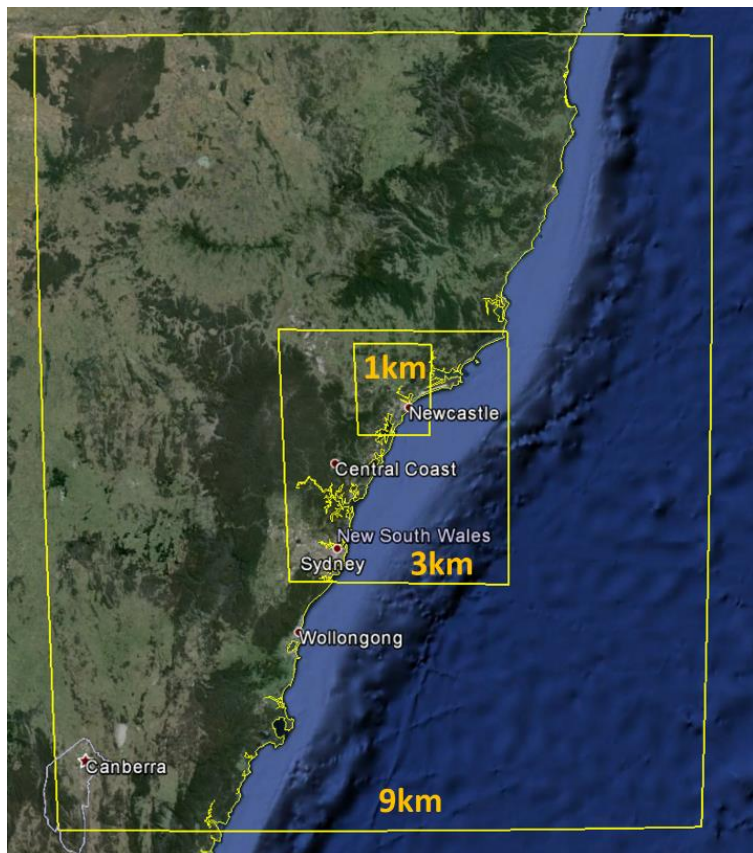


Figure 2. Map showing positions of the 9 km, 3 km and 1 km modelling grids.

The usual practice is to centre each of the grids on the receptor site of interest, which in this case is Beresfield. However the 3-km grid has been extended to the south to include the Sydney Metropolitan Region as it is expected that the Sydney emissions will impact the Lower Hunter region. The 3-km grid is also extended on the western boundary to include the power stations and other sources in the Upper Hunter to account for their contributions to airborne particles in the Lower Hunter. The 1-km grid centred on Beresfield includes the Port of Newcastle, and the towns of Toronto to the south and Maitland to the north-west.

2.2 Meteorological module

The Cubic Conformal Atmospheric Model (CCAM) was used to predict meteorological fields including wind velocity, temperature, water-vapour mixing ratio (including clouds), radiation and turbulence (McGregor and Dix, 2008). CCAM was nudged at larger wavelengths towards 6-hourly European Centre for Medium-range Weather Forecasting (ECMWF) reanalyses using a scale selective filter, which was the smaller of two options being $\frac{1}{4}$ the width of the high-resolution area or 500 km. This configuration was designed to ensure that CCAM was able to use the detailed information in the ECMWF reanalyses. The meteorological fields force key components of the emissions and the chemical transport model, for example sea-salt

emissions are forced by wind speeds and some vehicle-based emissions have an evaporative effect forced by temperature. The meteorological module is key to the transport modelling process as chemical species are subject to transport and dilution within the model grids at rates determined by the wind direction, wind speeds and heights of the planetary boundary layer. The ability of CCAM to predict meteorological variables has been demonstrated previously during the Sydney Particle Study (Cope et al., 2014), modelling mercury in the Latrobe Valley (Emmerson et al., 2015) and during the air quality model ensemble project (Emmerson, 2014).

Meteorology from the UK Met Offices' global Unified Model (UM) was also examined for the November case study to compare with the output from CCAM (<http://www.metoffice.gov.uk/research/modelling-systems/unified-model>). The UM is designed to work on both climate and numerical weather forecasting timescales, and for global and downscaled regional applications (Walters et al., 2011). The November period (up to 22 November) coincided with the time period being run for the Forecast Demonstration Project¹, thus the UM results were not available for the July case-study days. An example of the comparison of predicted hourly temperature, wind speed and wind direction from CCAM and the UM modelling, with measurements from the Stockton air quality monitoring station, is shown in Figure 3. This demonstrates that CCAM models the observed meteorology with reasonable accuracy and that it performs as well, if not better at times, than the UM, which is one of the global state-of-the-art meteorological models. Predicted peak temperatures from CCAM are slightly higher than observed and lead to slightly increased chemical activity, particularly for secondary organic aerosol production. The wind speeds for both CCAM and the UM are high at Stockton due to its proximity to the coast.

A requirement for this study is to compare meteorology with NSW air quality monitoring station data. Sites selected for air quality monitoring are chosen because there is a need to measure pollutants such as ozone and NO_x at a location, but not on their representativeness with regard to the meteorology of the locale. Thus these monitoring sites are usually situated in built-up areas, not in open locations where there is a long fetch. Modelling of meteorology relies on maps of the land surface roughness, thus the resolution of the models cannot evaluate individual street canyons and detailed circulation patterns within urban areas.

Wind roses are plotted for the whole modelling periods and compared with the observed wind speed and direction data at Newcastle, Stockton, Mayfield and Beresfield. Figure 4 shows comparison for 1–15 July, and Figure 5 shows comparison for 10–22 November. OEH monitoring was only established at Mayfield in August 2014 and therefore there are no measurements for July at Mayfield. In general the predicted wind direction is good, though modelled wind speeds are more indicative of open ground with a longer fetch, as expected. In November, when the wind direction is from the south-east (from the sea), very high winds are predicted at Stockton. The 1-km model grid cell at Stockton is right on the coast, therefore higher wind speeds are predicted here as the surface roughness will represent the sea.

¹ The Forecast Demonstration Project was funded by OEH and the Rural Fire Service and predicted meteorology and air quality during 2015. See abstract by P. Steinle et al at the 9th annual CAWCR workshop in 2015 http://www.cawcr.gov.au/static/technical-reports/CTR_080.pdf.

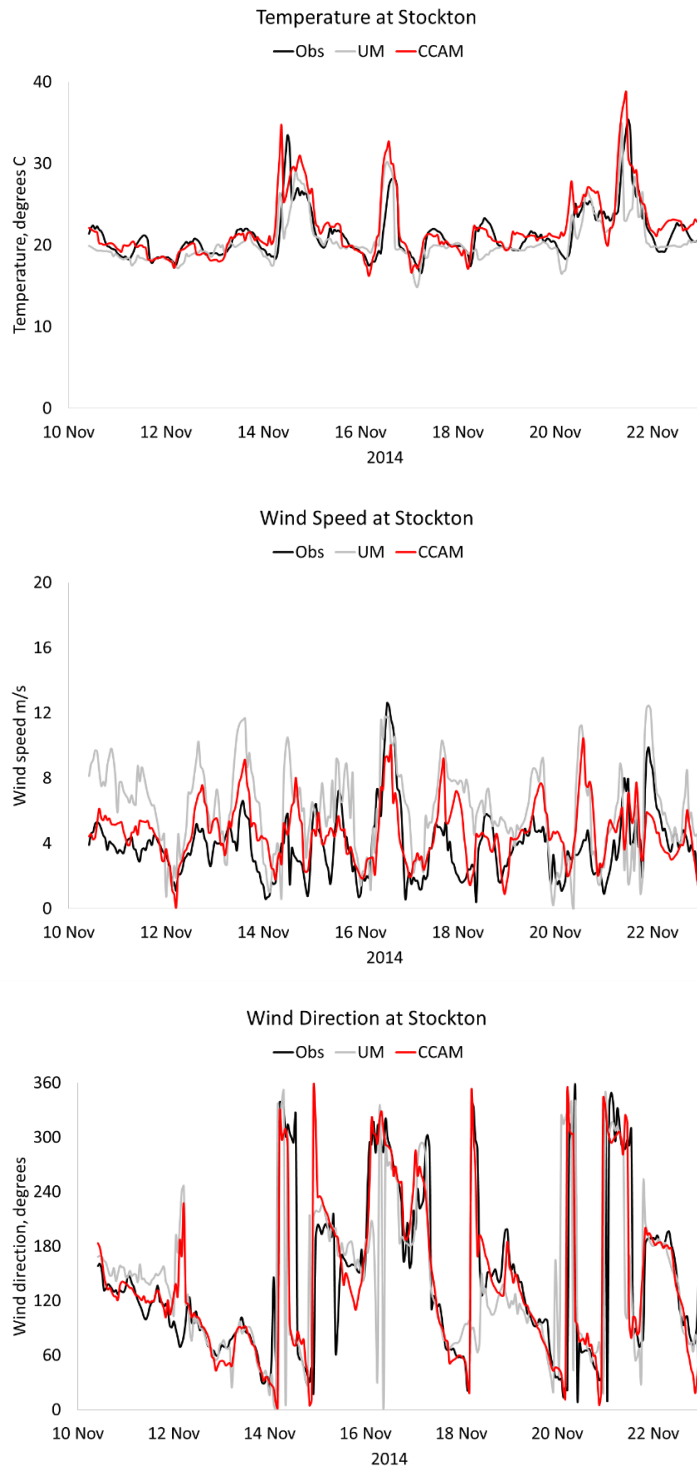


Figure 3 Comparison of measured temperature, wind speed and wind direction at Stockton with model output from CCAM and the UM.

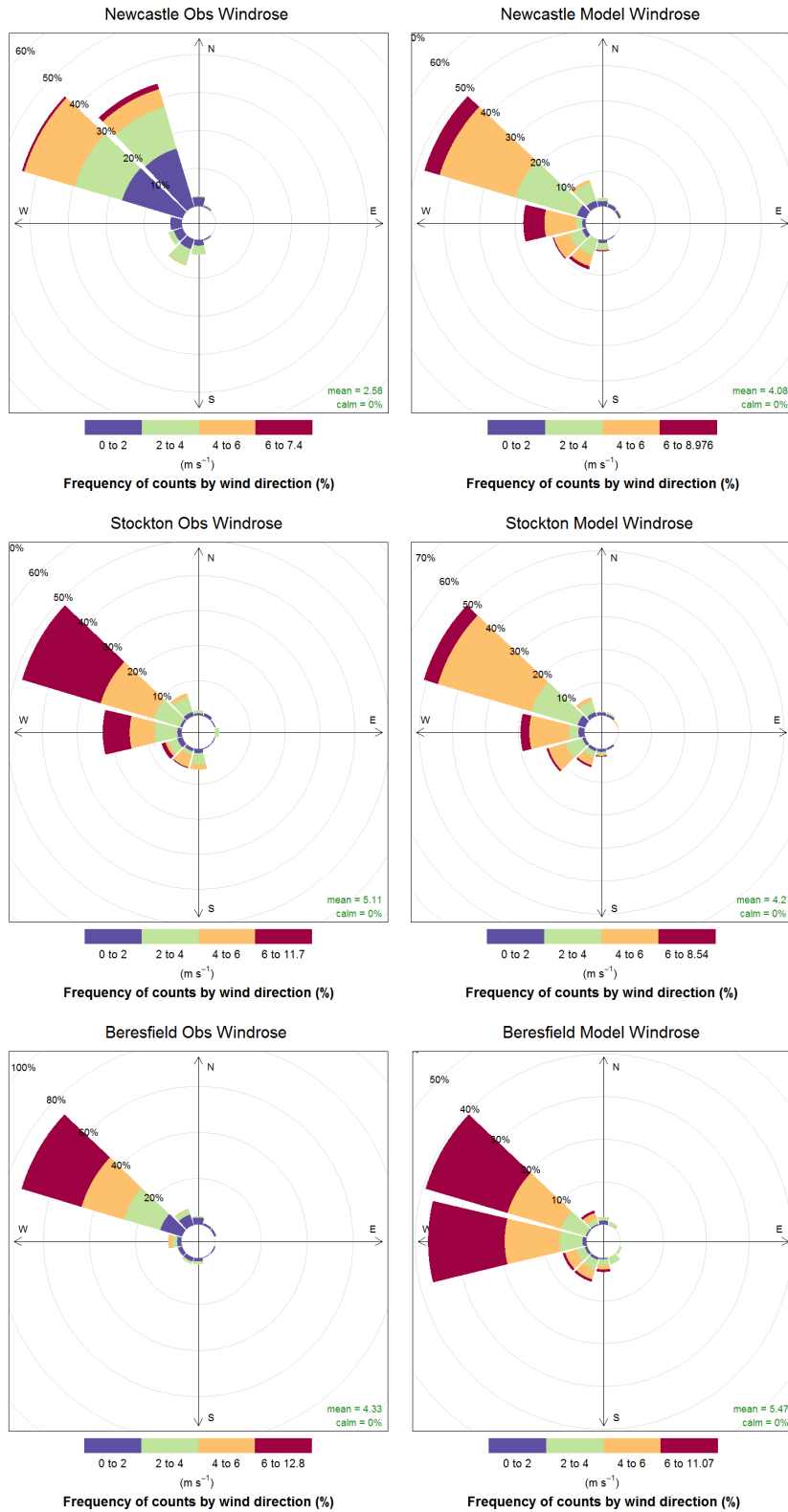


Figure 4 Wind roses for Newcastle, Stockton and Beresfield for 1–15 July 2014. Observed data is on the left, modelled predictions from CCAM are on the right.

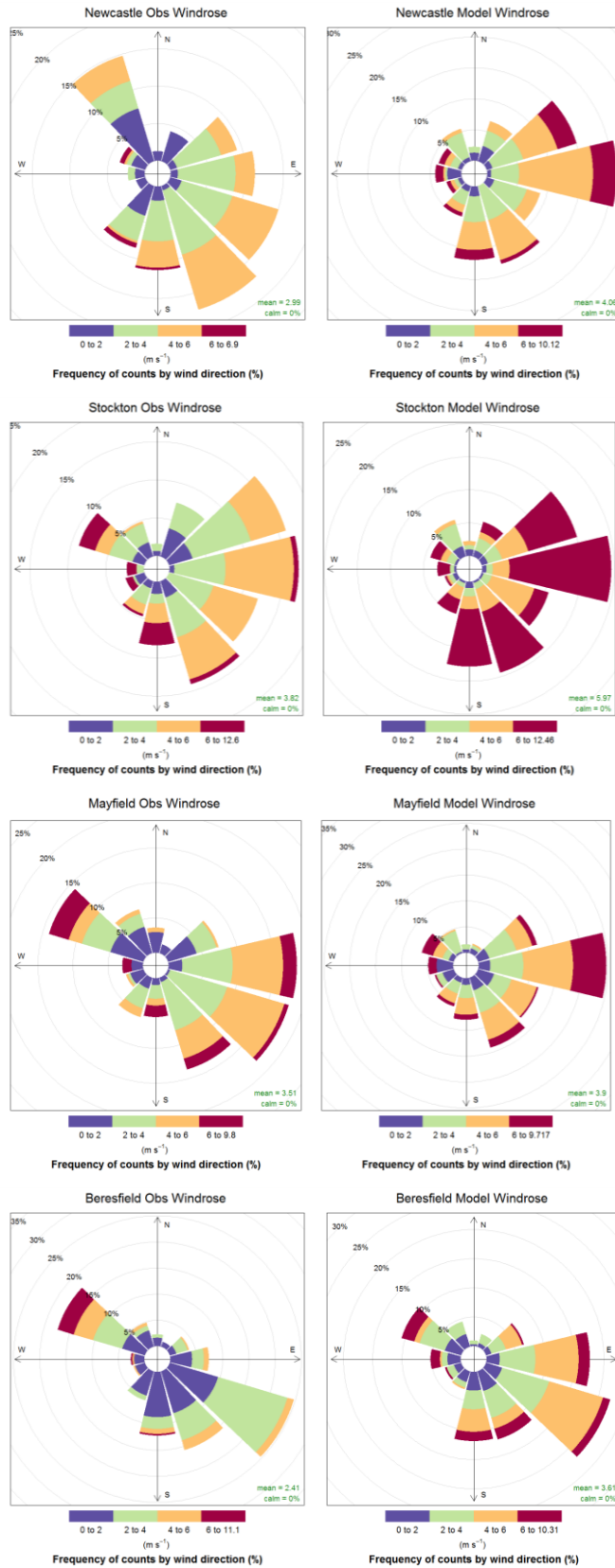


Figure 5 Wind roses for Newcastle, Stockton, Mayfield and Beresfield for 10–22 November 2014. Observed data is on the left, modelled predictions from the UM are on the right.

Metrics have been calculated for temperature and wind components in Table 1. As wind direction is a radial measurement, the easterly and northerly vectors of the wind must be calculated to perform statistical comparisons. The vectors take into account speed and direction. The mean bias (MB) and mean absolute gross error (MAGE) are calculated according to:

$$MB = \frac{1}{N} \sum_{i=1}^N (P_i - O_i)$$

$$MAGE = \frac{1}{N} \sum_{i=1}^N |P_i - O_i|$$

where N is the number of data points, P is the predicted value from the models and O is the observed value, at point i in time. The MB and MAGE (in variable units) give the difference between the modelled value and the observations. Where the value is negative this denotes that the average model value is lower than the average observed value. Table 1 also gives the r^2 correlation coefficient between model and observations.

Table 1 Metrics for temperature and wind components at the LHPCS sites. Measurements are compared to CCAM for 1–15 July and compared with the UM for 10–22 November 2014. MB – mean bias; MAGE – mean absolute gross error

		Newcastle		Stockton		Mayfield		Beresfield	
		Jul	Nov	Jul	Nov	Jul	Nov	Jul	Nov
Temperature	MB, °C	0.16	-0.26		-0.76		0.10	0.03	-0.45
	MAGE, °C	1.50	1.27		1.54		1.75	1.98	1.92
	r^2	0.76	0.73		0.48		0.77	0.65	0.76
Easterly Vector	MB, m s ⁻¹	1.55	-0.69	-0.76	-1.48		-0.44	1.07	-1.12
	MAGE, m s ⁻¹	1.91	1.63	2.12	2.50		1.49	1.99	1.79
	r^2	0.27	0.60	0.24	0.51		0.58	0.39	0.55
Northerly Vector	MB, m s ⁻¹	0.70	-0.23	0.37	0.66		-0.03	1.01	0.50
	MAGE, m s ⁻¹	1.50	1.46	1.36	1.99		1.31	1.62	1.36
	r^2	0.30	0.53	0.41	0.65		0.46	0.25	0.55

Temperature is predicted better by both models than the wind components, shown by the lower MB and high r^2 values. The mean bias in temperature is less than 0.8°C with a mean absolute gross error of less than 2°C. The bias in the easterly and northerly wind components is less than 1.55 m s⁻¹ with a mean absolute gross error of less than 2.5 m s⁻¹.

2.3 Emissions module

Anthropogenic emissions were obtained from the 2008 Sydney Greater Metropolitan Region inventory produced by the NSW Environmental Protection Authority (available at <http://www.epa.nsw.gov.au/air/airinventory2008.htm>). These emissions were provided by the NSW Office of Environment and Heritage for modelling purposes as point sources or area sources at 1 km resolution for 15 different source categories, listed in Table 2. Note that GMR Emission Inventories are compiled every five years, with the 2013 base case year emissions inventory not yet completed or published.

Table 2 List of source categories in the 2008 Sydney GMR inventory

Vehicular	Commercial – Domestic
Petrol exhaust	Aircraft
Diesel exhaust	Commercial vehicles
Other exhaust	Industrial vehicles
Petrol evaporative	Locomotive
Non-exhaust PM	Shipping
	Wood heaters
Industrial point sources	Other area-based sources
Coal power generation	
Gas power generation	
Other point sources	

The emission rates from each source group were split into species appropriate for the chemistry scheme in the model, discussed in section 2.4. These species include volatile organic compounds (VOCs), nitric oxide (NO), ammonia (NH₃), sulfur dioxide (SO₂), levoglucosan (smoke tracer) and particle-phase elemental and organic carbon. The particulate phase organic species are also split into volatility bins. Primary sulfate emissions are represented as a fraction of the SO_x, which for all but one category in Table 2 are calculated at 3% of the SO_x emission for each group. Shipping, however, uses a much higher sulfur content fuel that will yield higher primary sulfate emissions. Therefore the shipping category in Table 2 uses 33.5% primary sulfate as a function of the total PM₁₀ shipping emission.

The gridded locations of emission for some of these species are shown in Figure 6 for July 2008. Sources of SO₂ emission include power stations, aluminium smelters and shipping at the Port of Newcastle. Sources of ammonia (NH₃), organic carbon and levoglucosan exhibit similar spatial patterns and are aligned with populated areas. Ammonia and organic carbon are also released from industrial operations on Kooragang Island.

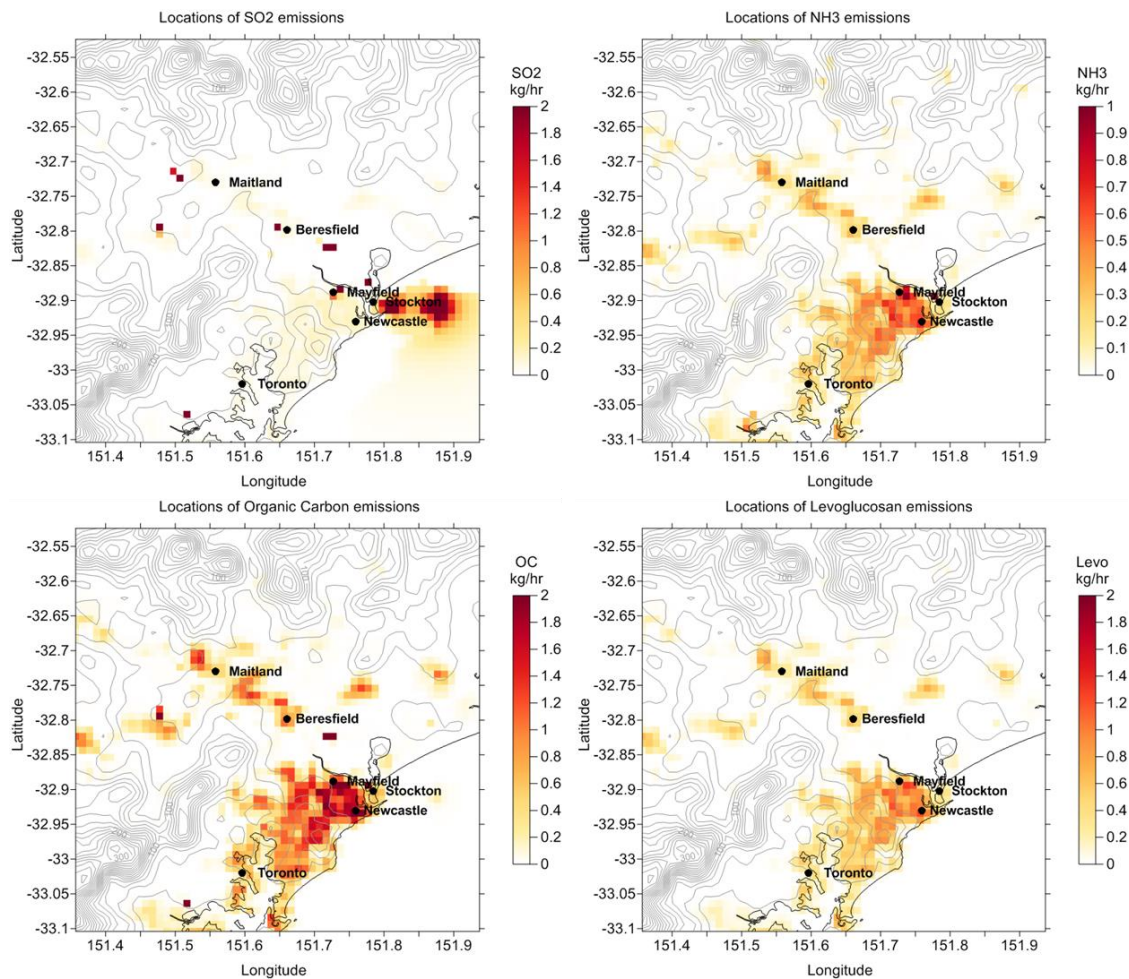


Figure 6. Emissions of SO₂, NH₃, organic carbon and levoglucosan for July from the 2008 GMR inventory. Note that maximum emission values for individual point sources greatly exceed the maximum values on the colour legends; the scale was selected to highlight the regional distribution of sources.

The anthropogenic emissions from the 2008 GMR emission inventory are not static and respond to changes in temperature and buoyancy of the atmosphere (plume rise). Point source emissions are varied on an hourly basis to represent operating conditions. Vehicular sources, including petrol evaporative use February 2008 base emissions, which are then scaled by the model temperature. Wood-heater emissions use the July 2008 base emissions and are varied during the year according to heating degree days, whereby residents are assumed to switch on their heaters once the 24-hour average temperature dips below 18°C. All other anthropogenic emissions groups use the base month appropriate to the model date. Similarly, natural emissions are calculated in line by the model specifically for the modelled periods, responding to temperature and wind speed conditions.

Natural emissions include biogenic VOCs from vegetation, wind-blown dust, smoke from fires and sea salt. The modelling framework includes methodologies for estimating emissions of VOC from vegetation (Azzi et al., 2012) and emissions of nitric oxide and ammonia from vegetation and soils. The framework also includes sea salt aerosol containing a wind-blown aspect (Gong, 2003) together with a shore-break mechanism which emits salt from surf zones around the coast (Clarke et al., 2003); emissions of wind-blown dust (Lu and Shao, 1999); and gaseous and aerosol

emissions from managed and unmanaged wildfires. Emissions from all but the wildfires are calculated inline in the CTM at each time step using the modelled meteorological fields for the study period. The fire emissions vary daily and come from the Monitoring Atmospheric Composition and Climate project GFAS (Global Fire Assimilation System) dataset (https://www.copernicus.eu/oper_info/global_nrt_data_access/gfas_fdp) and are speciated according to savannah burning conditions given in Andreae and Merlet (2001).

2.4 Chemical transport modelling

The chemical transport and particle dynamics modelling was undertaken using the CSIRO Chemical Transport Model (CTM) (Cope et al., 2004). The CTM is a three-dimensional Eulerian chemical transport model with the capability of modelling the emission, transport, chemical transformation, wet and dry deposition of a coupled gas and aerosol phase atmospheric system. Verification of CTM predictions for atmospheric pollutants such as NO, ozone (O₃) and particulate matter has been undertaken in previous studies (Azzi et al., 2013; Cope et al., 2014).

Concentrations of gas and particulate-phase species at the model grid boundaries were derived from a global run of the United Kingdom Chemistry and Aerosol scheme (UKCA) for the UK Met Office Unified Model (http://www.ukca.ac.uk/wiki/index.php/Main_Page).

The chemical transformation of gas-phase species was modelled using an extended version of the Carbon Bond 5 mechanism (Sarwar et al., 2008) with updated toluene chemistry (Sarwar et al., 2011). The mechanism was also extended to include the gas phase precursors for secondary (gas and aqueous phase) inorganic and organic aerosols. Secondary inorganic aerosols were assumed to exist in thermodynamic equilibrium with gas-phase precursors and were modelled using the ISORROPIA-II model (Fountoukis and Nenes, 2007). Secondary organic aerosol (SOA) was modelled using the Volatility Basis Set approach (VBS) (Donahue et al., 2006). The VBS configuration is similar to that described in Tsimpidi et al. (2010). The production of S-VI in cloud water was modelled using the approach described in Seinfeld and Pandis (1998).

The model was run for the July and November case-study periods with a 10-day spin up time to allow the processes in the model to settle from their initial conditions.

3 Results

The modelled-measured agreement will be described as ‘reasonable’ if the difference between the predicted and observed concentrations is within a factor of 2, and ‘very good’ if the results agree to within 50%.

3.1 Total PM_{2.5}

24-hour averaged PM_{2.5} is shown for each of the LHPCS sampling sites in July 2014 in Figure 7.

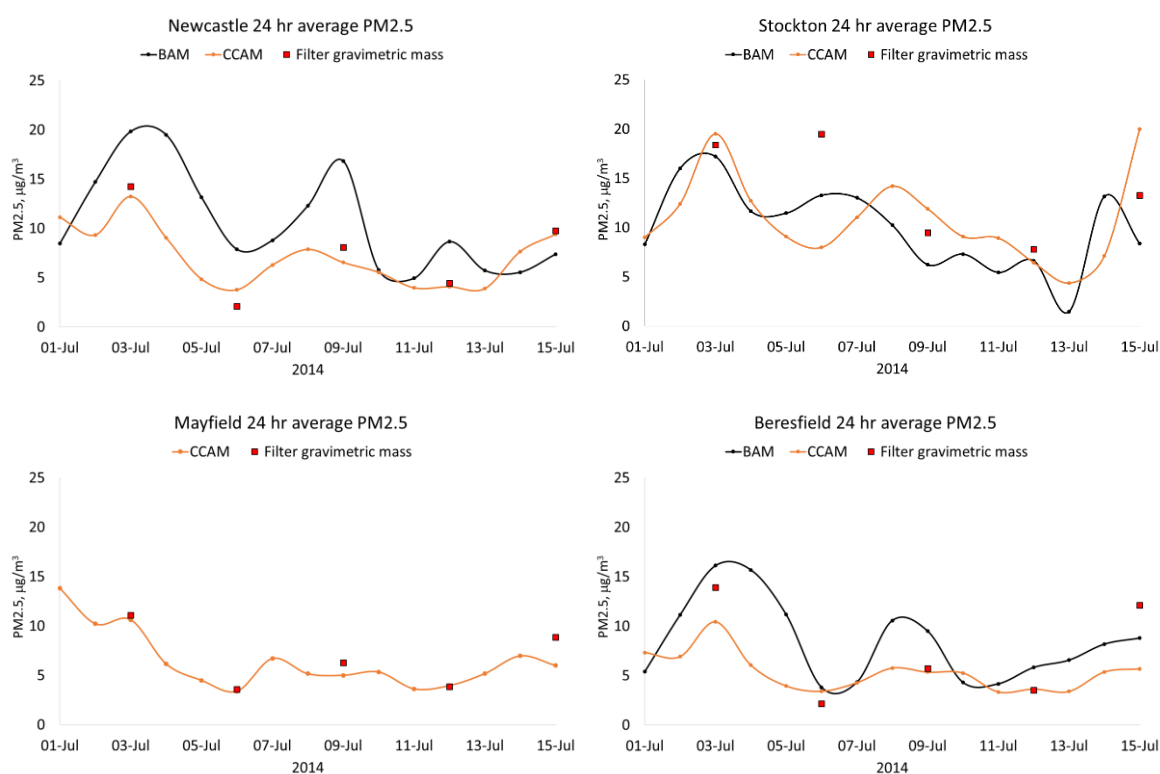


Figure 7 Modelled and observed 24 hour averaged PM_{2.5} at each of the LHPCS sites for July 2014. The filter samples were only collected every third day.

Modelled total PM_{2.5} is compared with the gravimetric mass from the filter samples taken every third day during the LHPCS measurement campaign, and also with continuous PM_{2.5} measurements from air quality monitoring stations at these sites. Data from the monitoring stations is not shown when the amount of valid data on a day is below 75%. Note that the model predicts dry aerosol, thus no moisture has been added to the gravimetric filter samples. For the July period the continuous measurements at Newcastle and Beresfield are from the OEH Air Quality Monitoring Network with PM_{2.5} measured using Beta Attenuation Monitors (BAM). For Stockton reference is made to continuous PM_{2.5} data from BAM monitoring at Orica’s Stockton air quality monitoring station for the July period. The BAM data is adjusted to ambient

temperature and pressure conditions, resulting in an average decrease of $0.3 \mu\text{g m}^{-3}$ in July and $0.8 \mu\text{g m}^{-3}$ in November. OEH monitoring of $\text{PM}_{2.5}$ was only established at Mayfield in August 2014 and therefore there were no BAM data for July at Mayfield.

The overall agreement between the model and observed filter values is very good; two-thirds of the points agree to within 25% and the maximum deviations are within a factor of 2. The differences between the BAM and filter values provide an indication of the uncertainty in the measurements. In the LHPCS $\text{PM}_{2.5}$ concentrations were determined based on gravimetric analysis of the filters from the ANSTO Aerosol Sampling Program (ASP) $\text{PM}_{2.5}$ cyclone samplers. The OEH BAMs determine the gravimetric mass based on attenuation of beta radiation through the filter in an automated process to provide continuous, real-time measurements.

The 24-hour averaged $\text{PM}_{2.5}$ comparison for November 2014 is shown in Figure 8, with modelled concentrations compared to 1-in-3-day LHPCS sampled concentrations and continuous BAM measurements from OEH operated air quality monitoring stations at all four sites (the industry-funded, OEH-operated Stockton and Mayfield air quality monitoring sites having been established by this time). In this case results from both the CCAM and UM driven models are compared with the observations. The UM run shows better agreement with both sets of observations than CCAM. The over-prediction in CCAM increases towards the end of November, caused by an over-prediction in the organic matter component, due in part to the modelled impact of fires in north-west Australia (Figure 9). The modelled secondary organic aerosol produced from the smoke plume extends right across Australia to New South Wales and causes an average background concentration in the Lower Hunter region of up to $8 \mu\text{g m}^{-3}$. It appears that the model is likely to be over-predicting the impact of these fires. The high transfer of smoke emissions to secondary organic aerosol may be caused by too low a volatility being set for smoke emissions in the volatility basis set (VBS) code, and this is being investigated further. This will have a bigger impact on SOA and thus $\text{PM}_{2.5}$ in summer when the higher temperatures cause chemistry to act faster. The response of the SOA system is temperature-dependent, so can vary on a day-to-day basis. At the end of November the model predicts more SOA, some of which is smoke-based and some is biogenic in origin, again due to temperature-driven emissions.

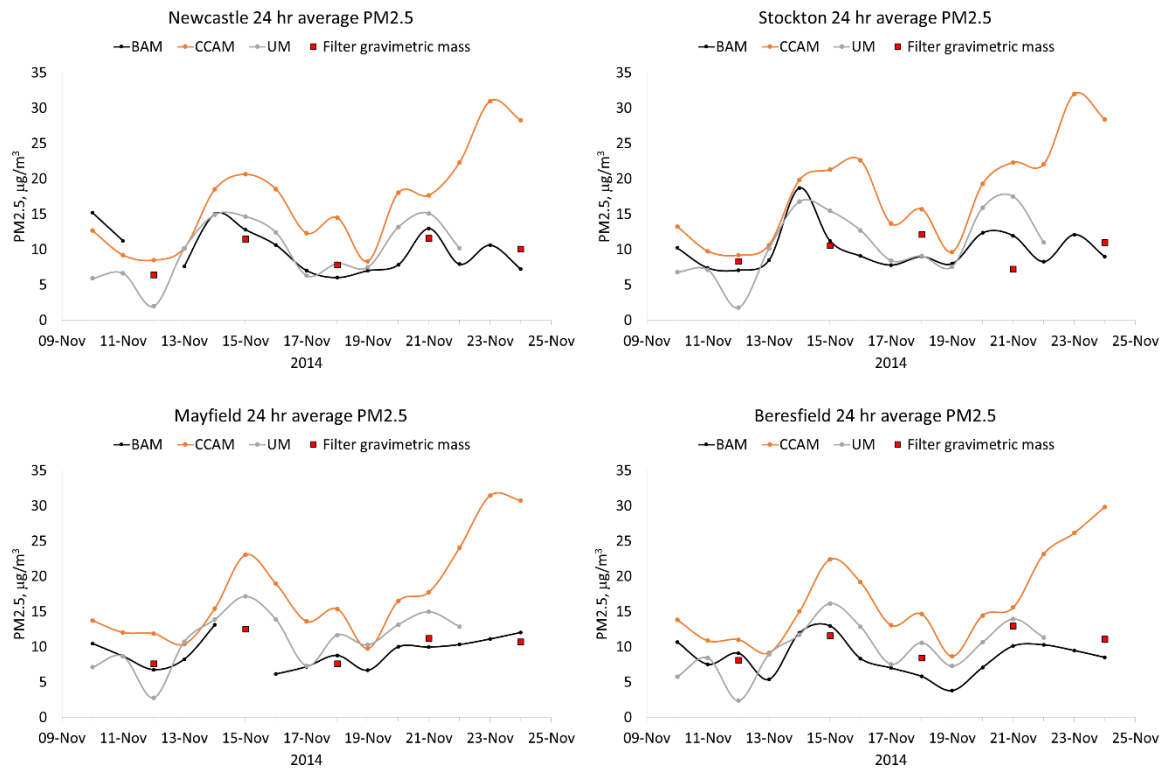


Figure 8 Modelled and observed 24-hour averaged $PM_{2.5}$ at each of the sites for November 2014. The filter samples were only collected every third day.

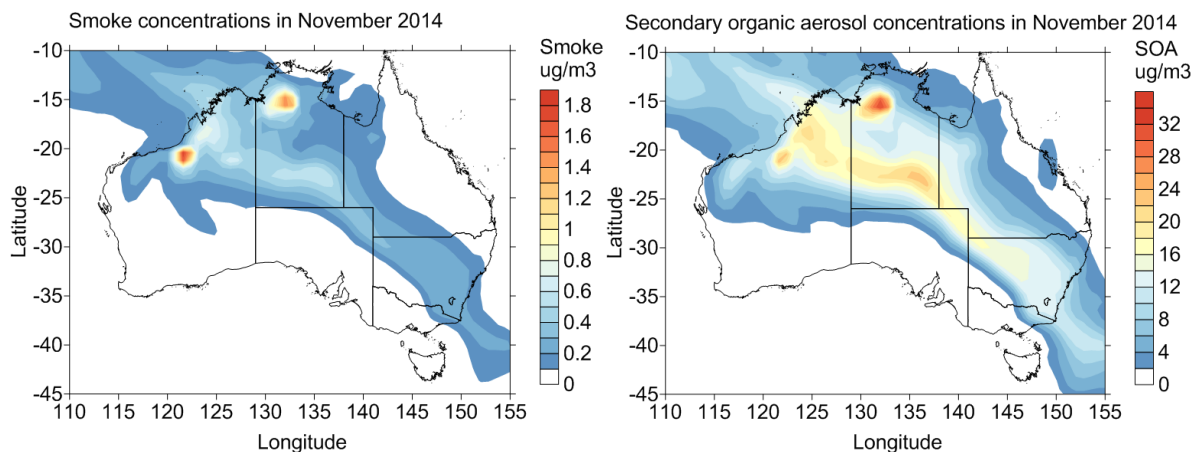


Figure 9 Modelled concentrations of smoke and the secondary organic aerosol produced from the smoke emissions on the Australia-wide grid from CTM using CCAM meteorology.

3.2 $PM_{2.5}$ components

Bar charts of the contribution of each modelled particulate component at the $PM_{2.5}$ size fraction are shown in Figure 10. Note that these are only the measured components of $PM_{2.5}$ that correspond to modelled species; there are many other species that make up the total $PM_{2.5}$ shown in Figure 7 and Figure 8. The model does

not explicitly predict concentrations of the following measured species, accounting for them as part of other lumped species: aluminium, silicon, phosphorus, titanium, vanadium, chromium, manganese, iron, cobalt, nickel, copper, zinc, selenium, lead, bromide, oxalate, fluoride, acetate, formate, methanesulfonate, arbatol, mannosan, mannitol, galactosan and glucose.

The components shown are: sodium (Na), chloride (Cl), potassium (K), magnesium (Mg) and calcium (Ca) (all components of sea salt), ammonium (NH₄), sulfate (SO₄), nitrate (NO₃), levoglucosan (a wood-smoke tracer), elemental carbon (EC) and organic matter (OM). The bars in Figure 10 are arranged so that the contribution of each component from the observations is plotted to the left of the modelled predictions. In all cases, the averages only include the sample days, i.e. every third day from 3–15 July and 12–24 November 2014. In November there are two models to compare with the observations; CCAM and the UM. As the UM is only available up until 22 November, the average observed components have been calculated from 12–21 November inclusive.

In the analysis of model performance, model results are described as ‘reasonable’ when they lie within a factor of 2 of the measured averages. There are major aspects of the observations that the model has captured well, but there are also some where more work is needed to improve the modelling.

The sea-salt components sodium, Na and chloride, Cl have been predicted reasonably across the sites, although better for November than July when the model slightly over-predicted. Ammonium and nitrate were reasonably well predicted except at Stockton in winter, where the large under-prediction is due to a local source contributing ammonium nitrate at Stockton, which is not fully accounted for in the modelling. This point source emitting ammonium nitrate aerosol is located about 800 m from the Stockton site and is discussed more fully in the accompanying main report on the LHPCS by Hibberd et al. (2016). Furthermore, it should be noted that Eulerian models such as the CTM are unable to predict in-plume concentrations for plumes narrower than the inner grid-cell resolution (1 km in this study).

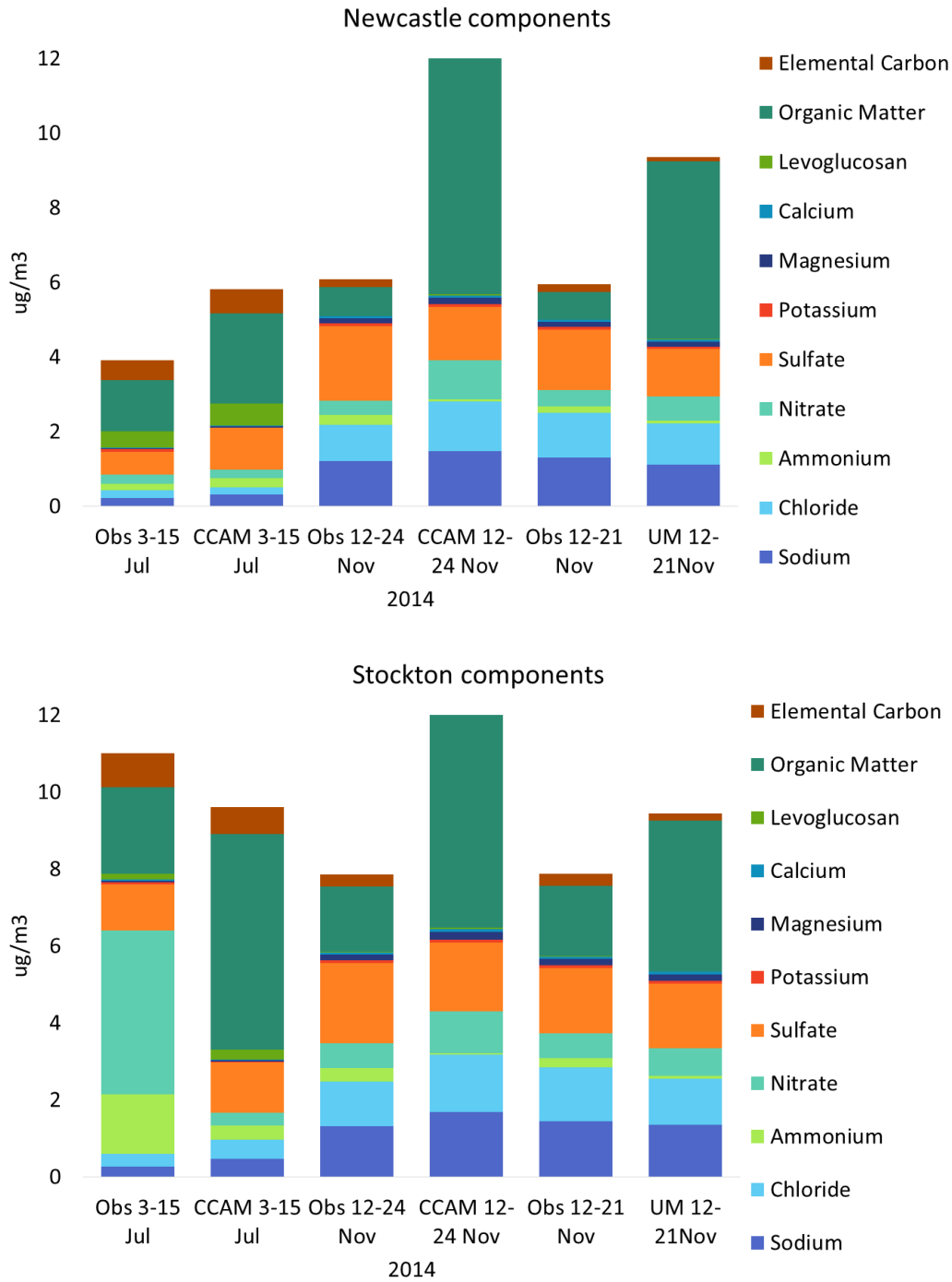


Figure 10 Comparison of measured and modelled component concentrations of PM_{2.5} for July and November 2014 at Newcastle, Stockton, Mayfield and Beresfield monitoring sites. Note that sum of components here do not equal total PM_{2.5}. Figure continues on next page.

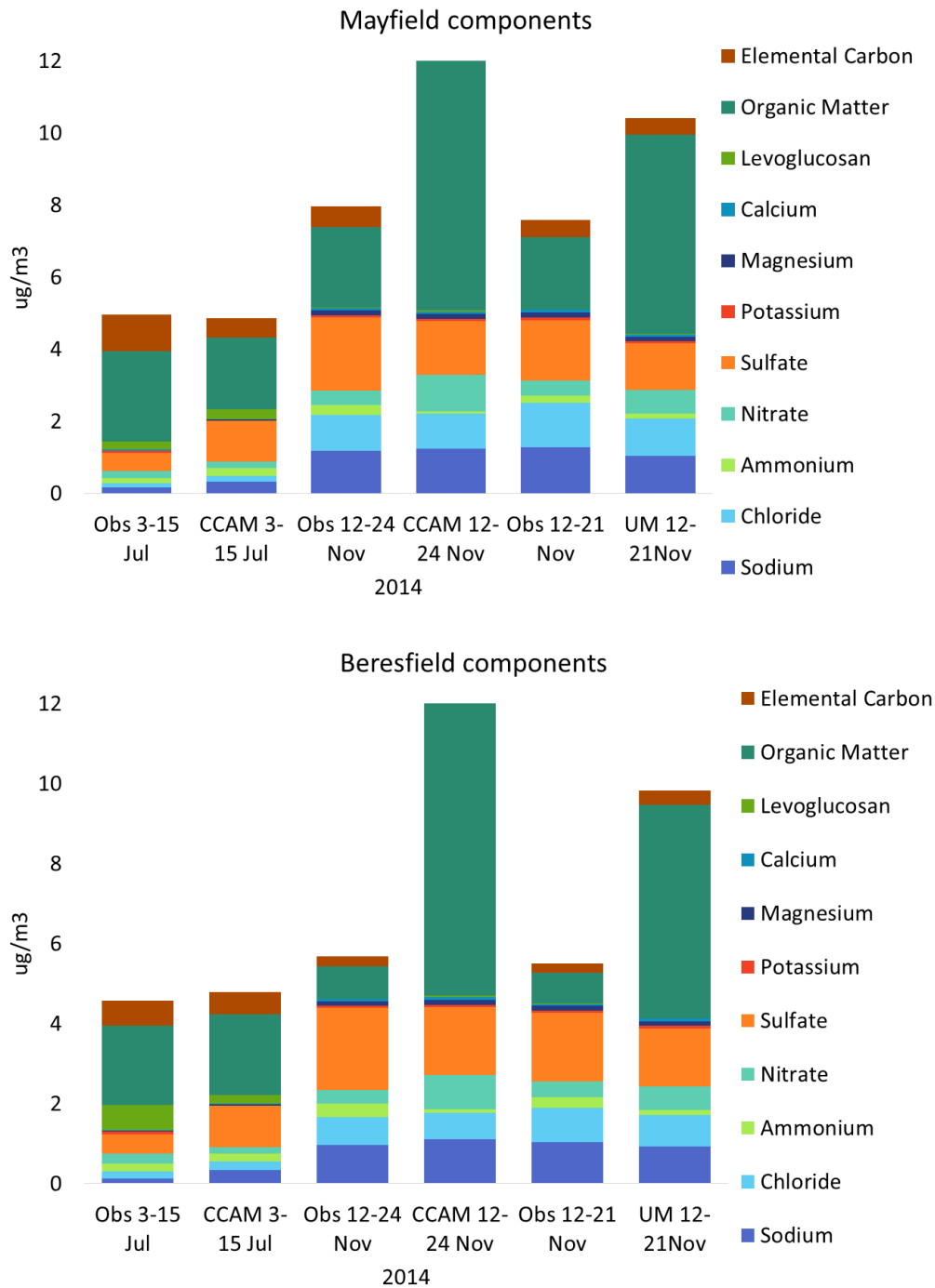


Figure 10 continued.

Levoglucosan is a wood-smoke tracer indicative of contributions from both residential wood heaters and from bushfires (although there is loss of levoglucosan as the smoke plumes age). The levoglucosan contribution has also been reasonably predicted during both periods, though it is on the low side in Beresfield in winter, indicating the difficulty of accurately modelling local domestic wood-heater use. The vegetation fires occurring west-south-west of Beresfield may also have contributed to the under-prediction. Sulfate aerosol is reasonably well modelled, but with a slight over-prediction in the winter case-study period. Organic matter is reasonably well modelled in winter except at Stockton where it is over-predicted. Organic matter is over-

predicted in summer, particularly by CCAM. As discussed above, this is mainly due to the over-prediction of the impact of fires in northern Australia, but influences from local burning events may also contribute.

In summary, when the summed concentrations for the selected components of PM_{2.5} are compared, the modelled total concentration at each of the sites in July is within 1-2 µg m⁻³ of the observations. This demonstrates that the chemical and physical processes in most cases are being reasonably predicted based on comparisons for most sites. At Stockton, the high ammonium nitrate in July is under-predicted and the organic matter has been over-predicted, so although the summed modelled and measured concentrations are similar the component concentrations differ. The UM and CCAM have modelled the main components in November reasonably well with the exception of organic matter which is over-predicted resulting in the summed modelled components being higher than the summed measured components.

3.3 Spatial variations

Given the overall reasonable agreement between the model and observations at the four monitoring sites, the model can provide information about the spatial variation in PM_{2.5} concentrations and key component of PM_{2.5} across the Lower Hunter region. As the UM model performed slightly better than CCAM for the component study in November, the UM model was used to create the November spatial contour maps shown in this section. Note that the whole modelled period has been used to create the spatial maps, not just the every third day 24-hour average period used by the LHPCS sampling. Each spatial map shows grey contour lines to mark the topographical features of the landscape and to show where the valley and coastline is located.

The modelled spatial distribution of PM_{2.5} and levoglucosan component are shown in Figure 11 for the July (left-hand side) and November (right-hand side) modelling periods. Based on the case-study periods considered, it should be noted that the LHPCS sampling sites are situated within the part of the Lower Hunter region where generally higher PM_{2.5} concentrations are predicted to occur. The four study sites generally cover the range of concentrations within this part of the region. Higher PM_{2.5} concentrations tend to occur in the more industrialised and populated areas. Elevated ground-level PM_{2.5} concentrations do not coincide spatially with industrial and power generation sources of PM_{2.5} and precursors of PM_{2.5} (e.g. SO₂ and NO_x) because emissions occur from tall stacks that take time to form secondary PM_{2.5} from precursor emissions.

Levoglucosan is elevated across the more populated regions in July. The major emissions source is domestic wood heating and these low-level emissions have the greatest impact locally. The November concentrations are negligible across the region. Although the fires in north-west Australia shown in Figure 9 generate levoglucosan, it reacts in sunlight to form other organic compounds, so it is not present when the fire plumes reach the Lower Hunter.

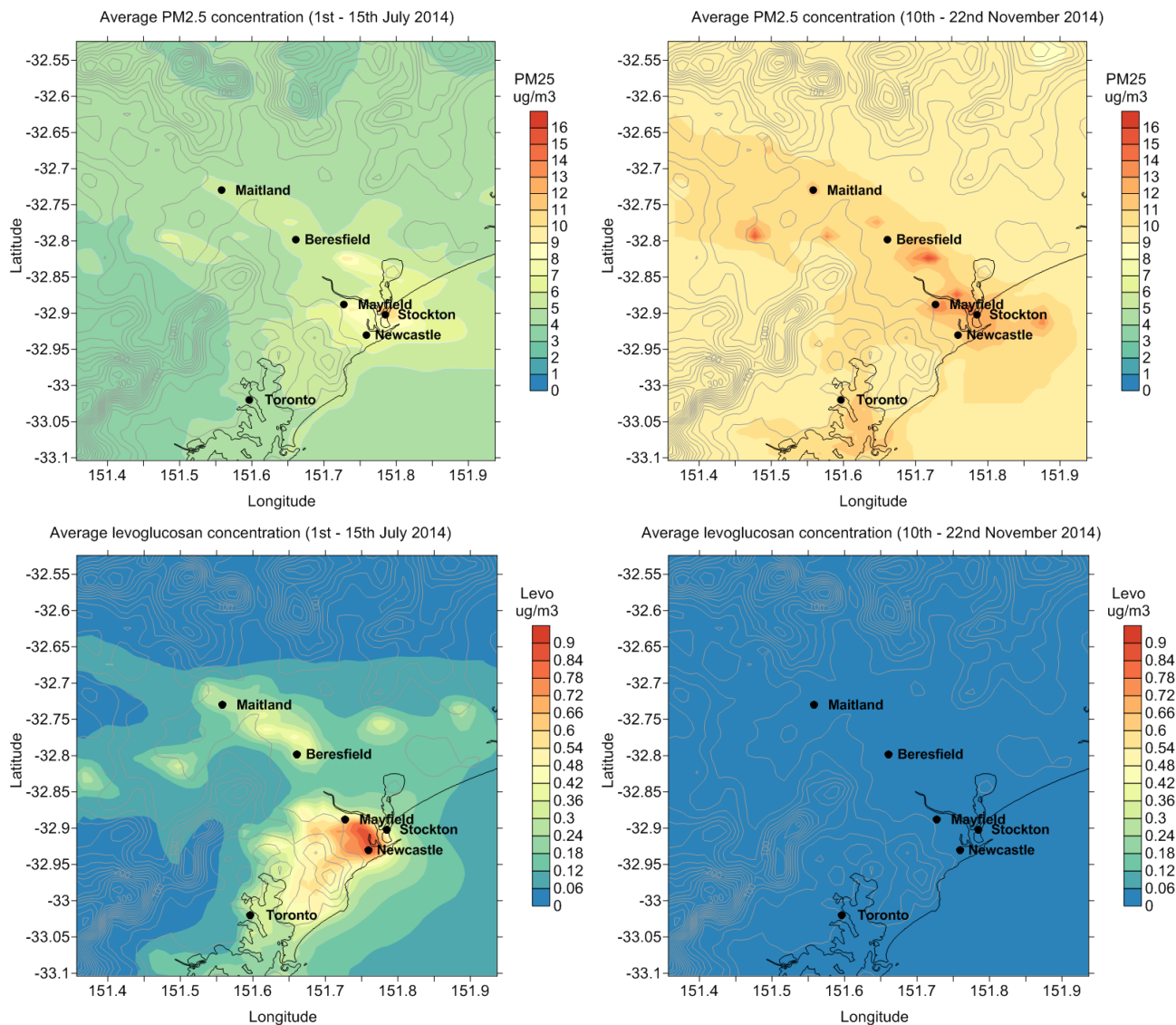


Figure 11 Spatial contour plots for modelled total PM_{2.5} and levoglucosan during (left) 1–15 July 2014 and (right) 10– 22 November 2014.

For elemental carbon and organic matter (Figure 12), the higher concentrations tend to occur over the more industrialised and populated regions. Background concentrations of elemental carbon away from these areas are similar in July and November. But this is not the case for organic matter, which shows higher concentrations in November due in part to the influence of the secondary organic aerosol discussed in connection with Figure 9.

Organic matter concentrations are both primary and secondary in origin and therefore are affected by transport processes. In July peak average concentrations reach no more than 4 $\mu\text{g m}^{-3}$ on the coast. In November the peak average concentrations exceed 8 $\mu\text{g m}^{-3}$ near the industrial point sources, but there is a high background concentration of 4 $\mu\text{g m}^{-3}$ due to the smoke transported from north-west Australia, shown in Figure 9. Higher concentrations of organic matter are expected in summer months as the increase in temperature causes chemical processes to act faster.

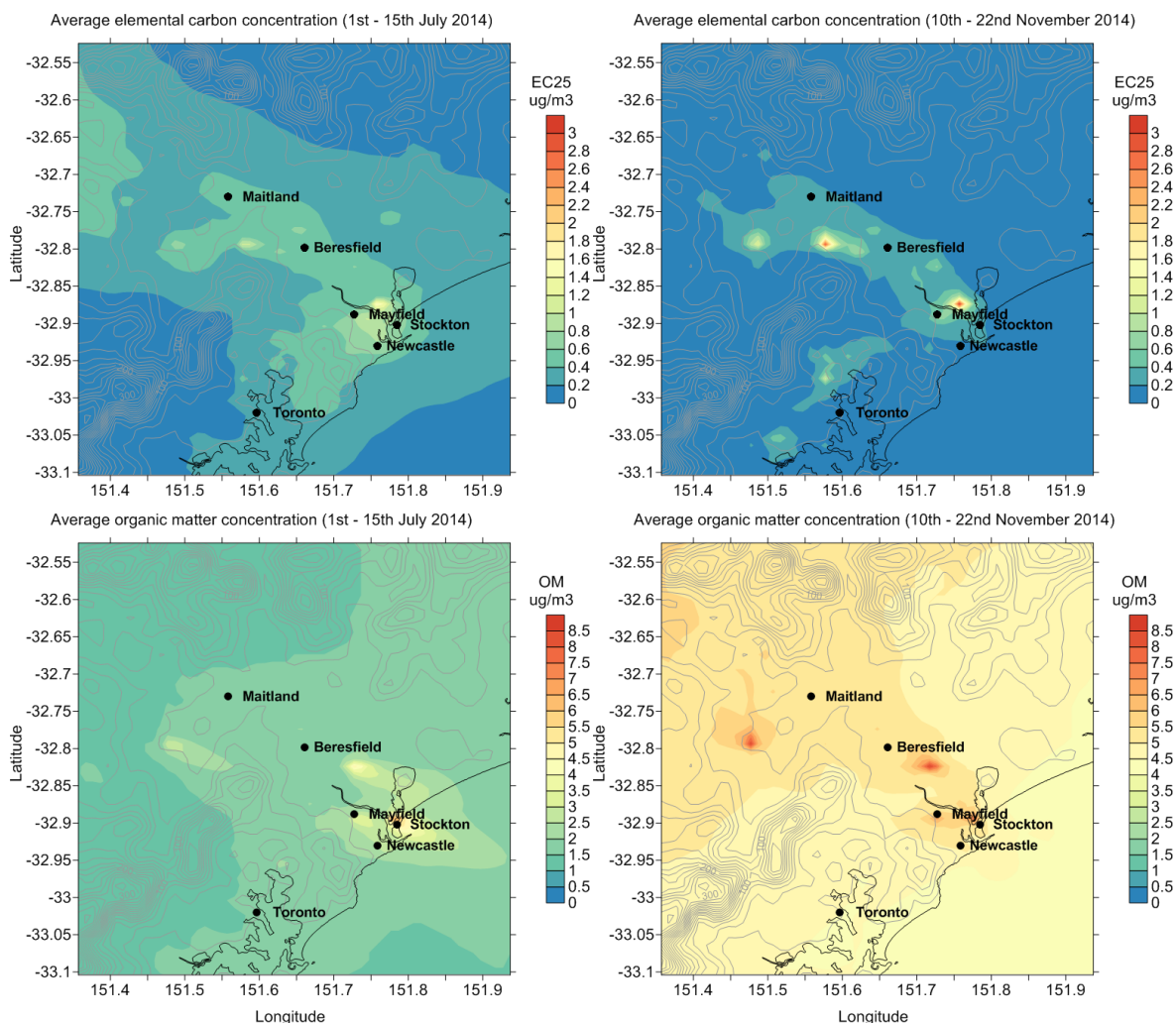


Figure 12 Spatial contour plots for modelled elemental carbon and organic matter during (left) 1–15 July 2014 and (right) 10– 22 November 2014.

Contour plots for sea salt and nitrate aerosol are shown in Figure 13. July concentrations of sea salt are lower than in November due to the predominant north-westerly winds in July. There is also little variation in sea salt concentrations across the land area in July; the sea salt in the PM_{2.5} fraction is transported across continental scales, so that its origin is probably the southern oceans. In contrast the November sea salt concentrations show a strong dependence on inland distance from the coast, with locally higher concentrations in regions with convoluted coastlines and so enhanced shore-break generation of sea-salt aerosol. This is evident at the Port of Newcastle and also for the Lake Macquarie area near Toronto. The locations of the higher nitrate concentrations are aligned with the locations of sea-salt shore-break emissions. Nitrate is related to sea salt, as sodium preferentially picks up nitrate when the sea salt ages. Therefore the higher concentrations of nitrate occur in summer and are located close to the coast. This suggests that the process encouraging nitrate out of the gas phase (HNO₃) occurs quickly and close to the point of emission.

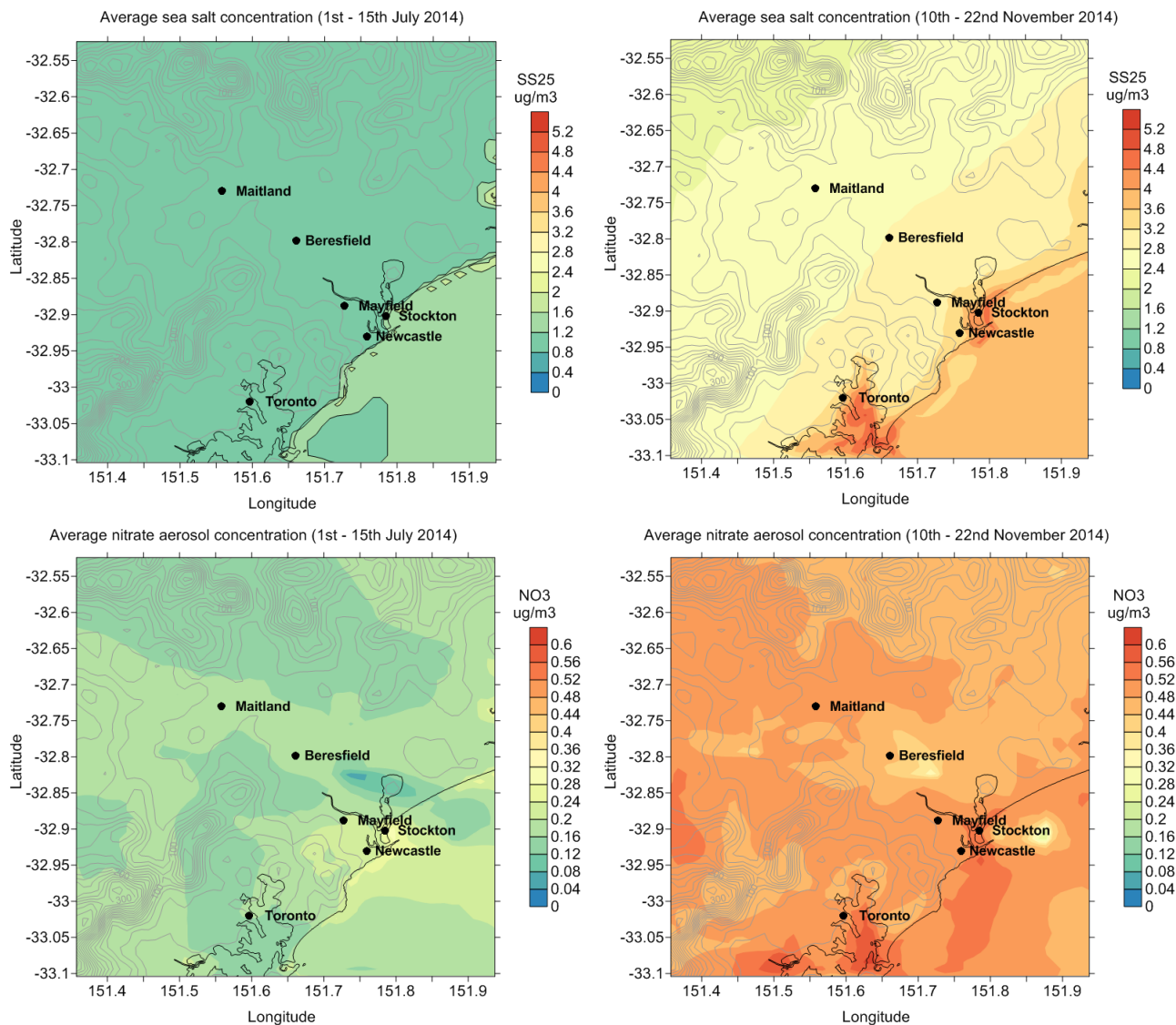


Figure 13 Spatial contour plots for modelled sea salt and nitrate aerosol during (left) 1–15 July 2014 and (right) 10–22 November 2014.

Ammonium and sulfate aerosol (Figure 14) are associated with each other with a significant component of secondary ammonium sulfate detected in the analysis of the LHPCS reported by Hibberd et al (2016). There is a localised source of sulfate east of Beresfield that corresponds with an industrial point source at Tomago. Note that the elevated SO₂ emissions from the power stations, as shown for example in Figure 6, do not show up directly as local ground-level sulfate aerosol, but are sources for sulfate aerosol detected throughout the airshed. The shipping emissions off the coast near Newcastle yield the peak sulfate aerosol in November, binding with ammonium. The competition between condensing ions ensures that the nitrate precursor gas, HNO₃ remains in the gas phase. This explains the much lower presence of nitrate aerosol near the Newcastle Port.

The dominant offshore wind direction is also seen in Figure 14. In July wind blows plumes from the north-west towards the sea. In the November period onshore flows are more prevalent.

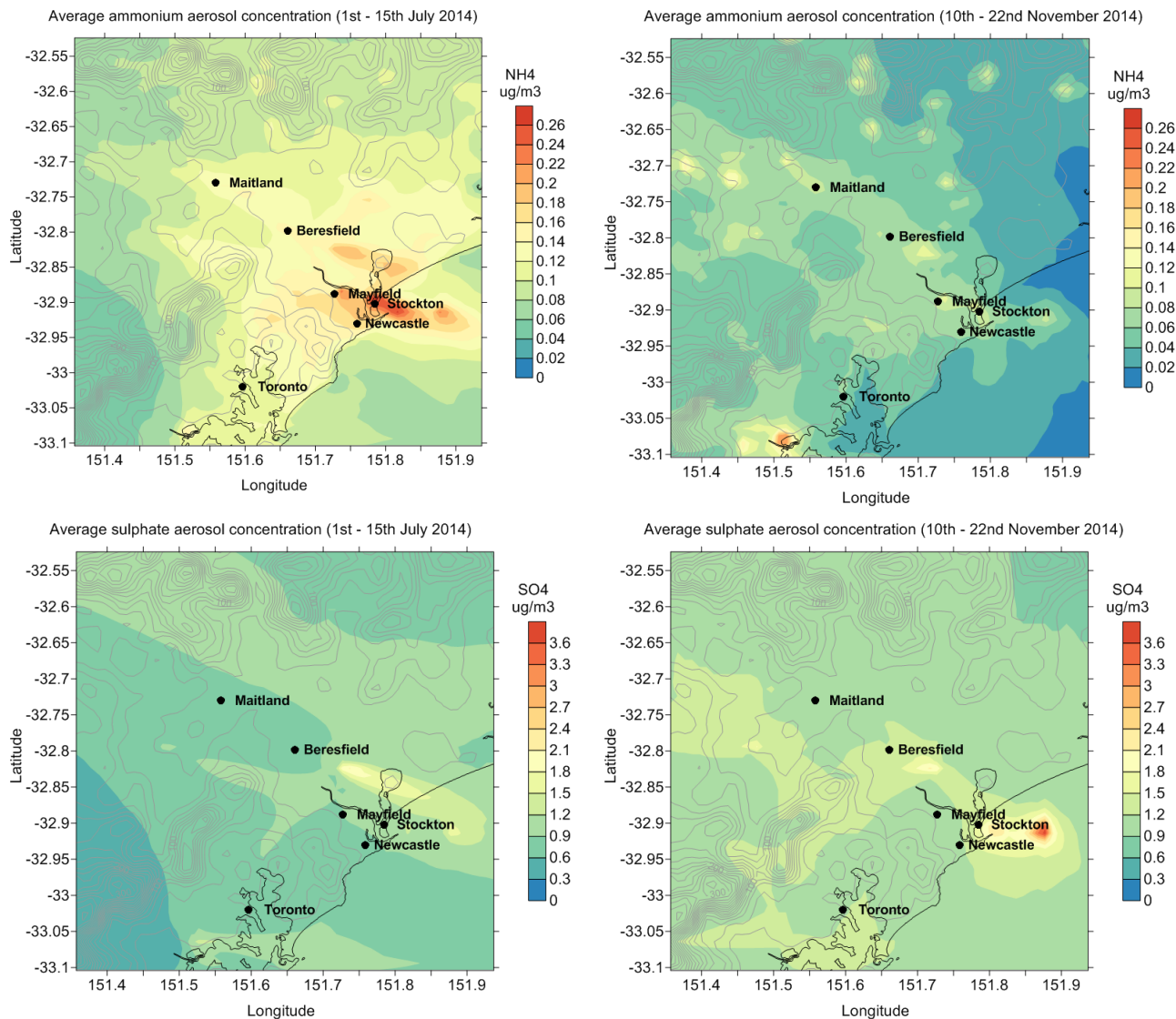


Figure 14 Spatial contour plots for modelled ammonium and sulfate aerosol during (left) 1–15 July 2014 and (right) 10– 22 November 2014.

3.4 Sources of the PM_{2.5} components

In addition to using contour plots of the spatial distribution of the PM_{2.5} components, it is possible to use bivariate plots for the modelled primary species data to assist in identifying the sources of predicted concentrations. Note that the bivariate plots show modelled hourly concentration, wind speed and wind direction data only. In the following figures the contour plots are accompanied by two polar bivariate plots, one centred on Beresfield, the other on Newcastle. Bivariate plots, created by Openair (Carslaw and Ropkins, 2012), show the concentration of a pollutant versus wind direction and speed. The bivariate plots show from which directions the highest concentrations of each pollutant come, and whether the pollutant is associated with low or high wind speeds. These can be used to identify the direction of sources and if they are generated for several locations, allow triangulation to determine pollution

source locations within the grid. In the plots presented in this section, the colour is the modelled pollutant concentration versus wind direction (angle) and wind speed (distance from centre).

Bivariate plots have been generated for PM_{2.5} components comprising only primary pollutants, i.e. they are emitted directly from sources rather than being formed in the air. Elemental carbon, sea salt and levoglucosan are primary components. Concentrations of secondary components of PM_{2.5} formed in the air from precursor pollutants are subject to chemical and transport processes and therefore bivariate plots are less useful for identifying sources of such components. Sulfate, nitrate and ammonium are mostly secondary components. Organic matter concentrations are both primary and secondary in origin and therefore are also affected by chemistry and transport processes.

The following figures are arranged so that each modelled pollutant is displayed for July in the left column and November in the right column for comparison. The spatial contour maps are also included again as a visual aid. Note that the pollutant concentration scale bars vary in magnitude across the bivariate plots presented. Also note that the whole modelled period has been used to create the bivariate plot, not just the every third day 24-hour average period available from the measurements.

Sea salt (Figure 15) shows lower concentrations in July than in November. This is expected as the onshore winds in summer bring the sea salt inland. In November the bivariate plots show the highest concentrations are observed to the south and east of Newcastle and Beresfield, corresponding to the high shore-break regions close to Newcastle and in the Lake Macquarie areas, with concentrations increasing as a function of wind speed. The polar bivariate plots show a 'source' to the west of both sites at speeds of 6–10 m s⁻¹. This does not represent a local source (there is no source visible in the spatial contour map), rather it is due to large-scale circulation bringing sea salt from the Southern Ocean when a southerly frontal change (with associated stronger winds) comes through the grid.

Elemental carbon (Figure 16) is a primary pollutant and concentrations are highest at low wind speeds (red areas in the figures close to the origin at low wind speeds). There are local sources of elemental carbon emissions present near both sites, which include vehicle emissions and residential wood heating (Hibberd et al., 2016). Low wind speeds reduce the dispersion of vehicle emissions resulting in higher concentrations. Levoglucosan is also a wood-smoke tracer (Figure 17). Residential wood-heating emissions are higher in the evening and early morning when wind speeds are lower due to overnight inversion conditions.

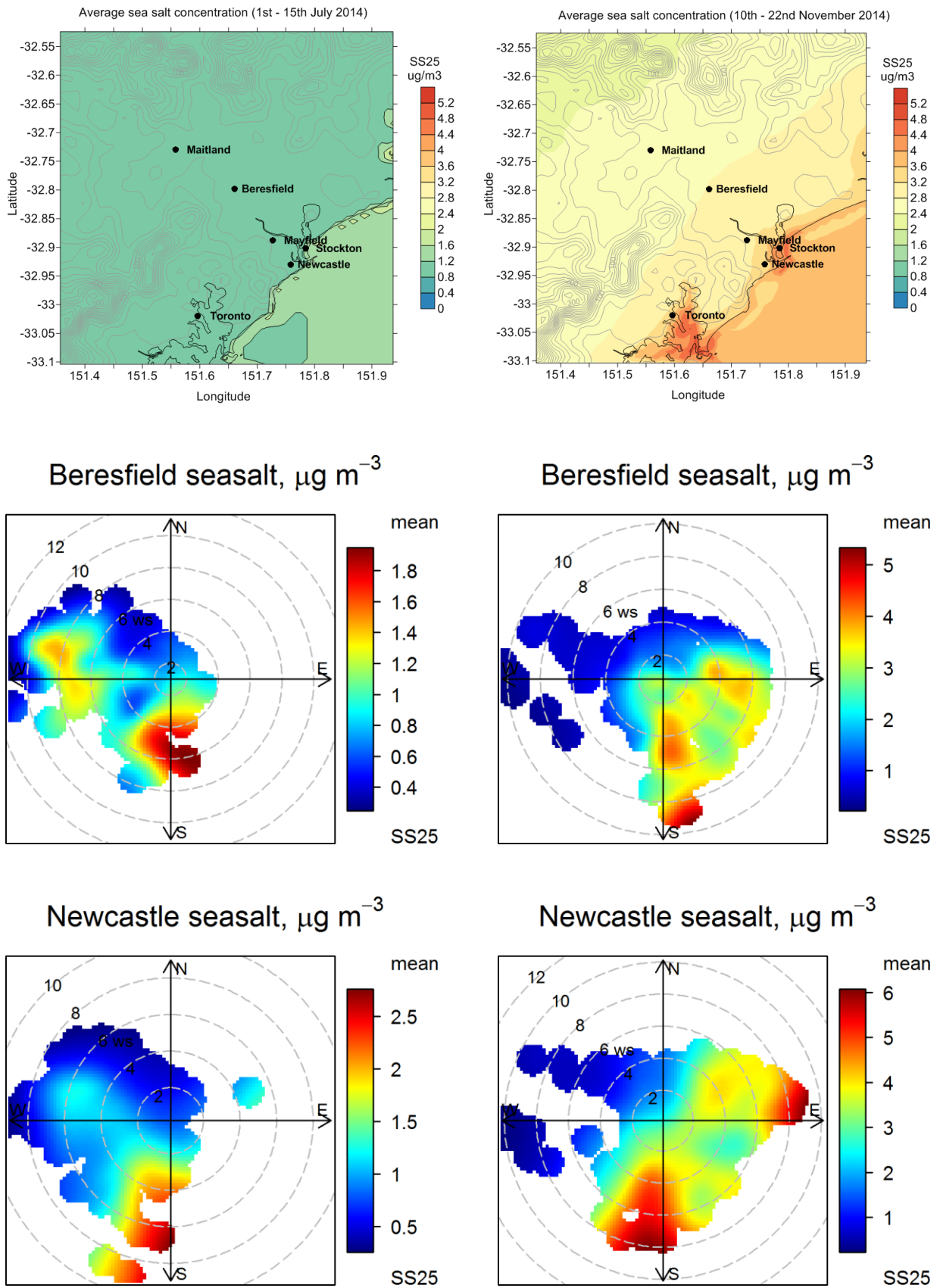


Figure 15. Spatial concentration and polar bivariate plots for modelled sea salt for July (left column) and November (right column).

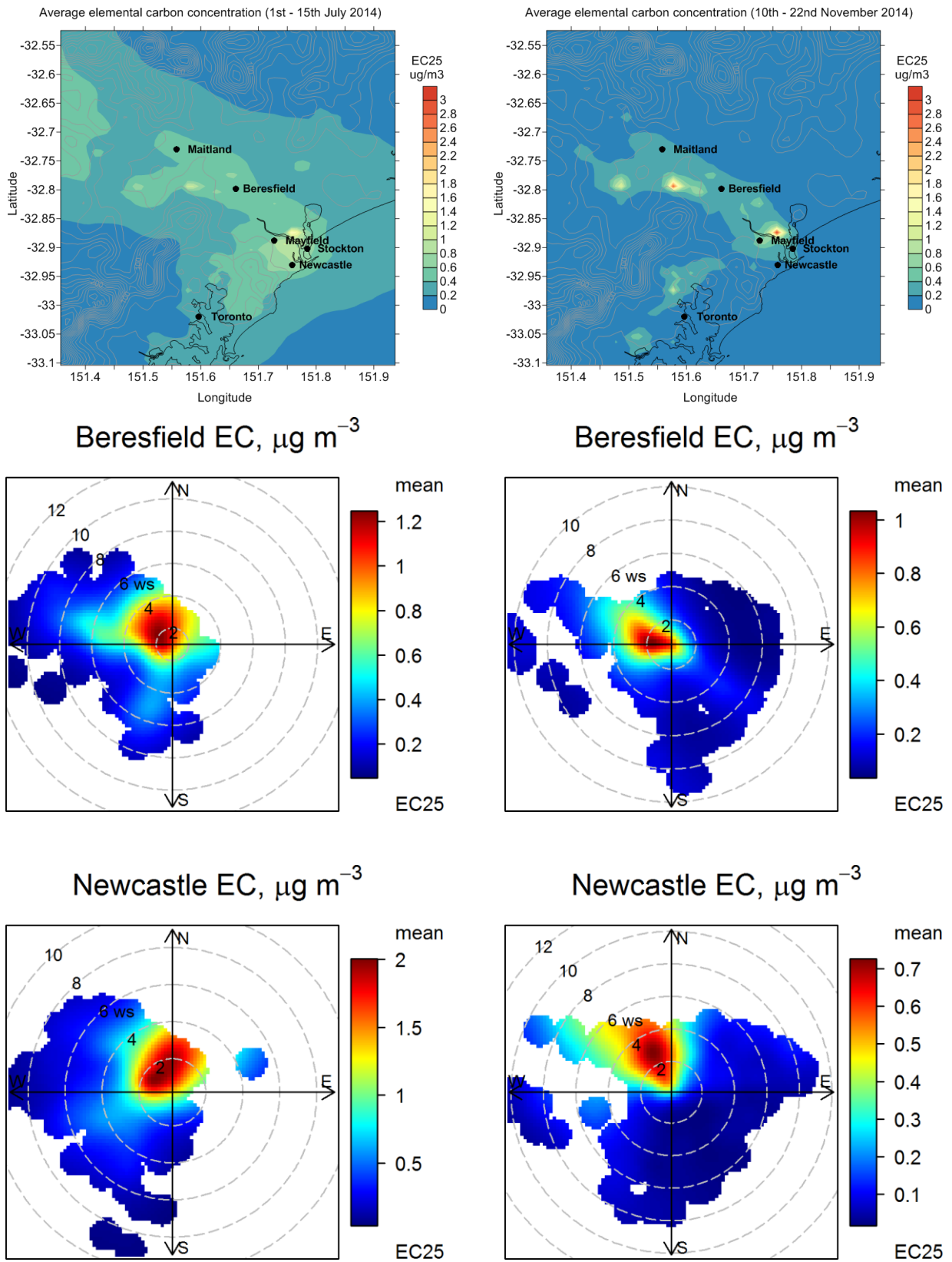


Figure 16. Spatial concentration and polar bivariate plots for modelled elemental carbon for July (left column) and November (right column).

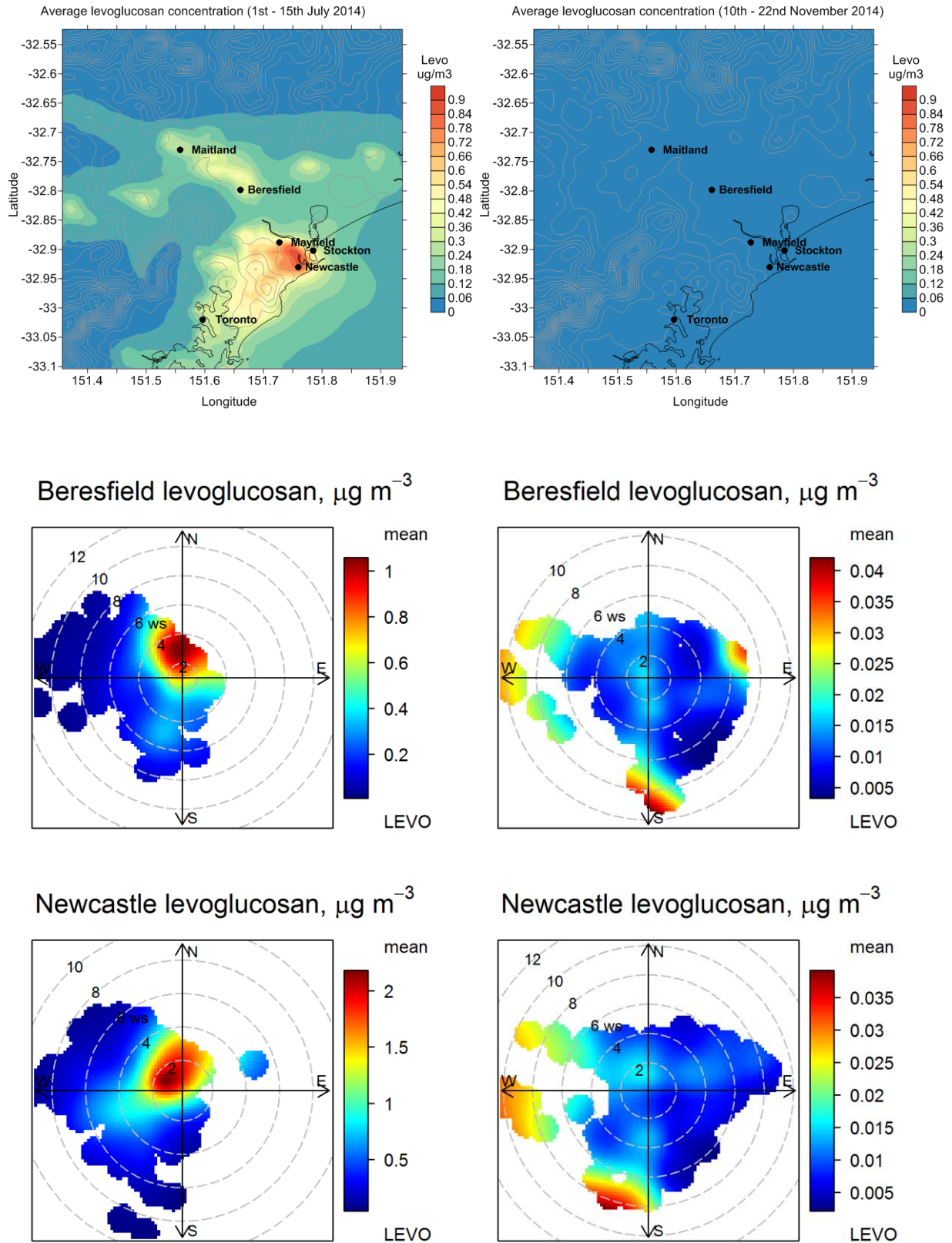


Figure 17 Spatial concentration and polar bivariate plots for modelled levoglucosan for July (left column) and November (right column).

The modelling predicts concentrations in 3D space and the fine-particle species breakdown can be extracted for any point on the grid. Therefore, component bar charts for non-measurement sites at Maitland and Toronto are shown for July and November from the model only in Figure 18. It must be assumed that the model caveats, such as the organic matter over-prediction, apply to these regions too. The locations of Maitland and Toronto are shown on the spatial contour maps in section 3.3.

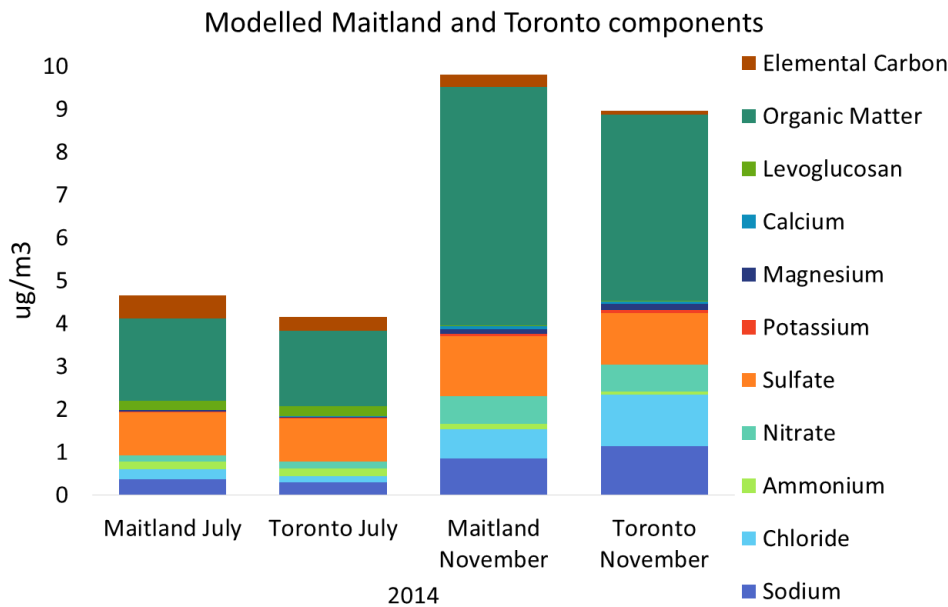


Figure 18 Modelled component concentrations of $\text{PM}_{2.5}$ for July and November 2014 at Maitland and Toronto. Note that sum of components here do not equal total $\text{PM}_{2.5}$.

Concentrations of all plotted components are approximately $4 \mu\text{g m}^{-3}$ higher than in July at both locations. There is more sea salt at Toronto in November which is expected as it is nearer to the coast than Maitland. Concentrations of individual components are similar for both locations during each modelled case-study period. There is slightly more organic matter predicted for Maitland than Toronto.

4 Summary

Chemical transport modelling was undertaken for two case-study periods in July and November 2014 to assist with analysis and interpretation of the Lower Hunter field campaign data. An opportunity to compare Unified Model meteorological predictions with the CSIRO CCAM model was used in November, as this period overlaps with the Forecast Demonstration Project which has been predicting real-time air quality concentrations in NSW airsheds.

The CTM predicted the measured aerosol components at the PM_{2.5} size fraction reasonably well for the July case-study period at the Newcastle, Beresfield and Mayfield sites. This demonstrates that the chemical and physical processes during this period are reasonably represented in the modelling. At Stockton, the high ammonium nitrate in July is under-predicted and the organic matter has been over-predicted, so although the summed modelled and measured PM_{2.5} concentrations are similar, the component concentrations differ. The under-prediction of ammonium nitrate at Stockton is due to a local source of direct ammonium nitrate emissions not represented in the emission inventory used for the modelling. This source is discussed in more detail in the main report (Hibberd et al., 2016). Furthermore, Eulerian models such as the CTM are unable to predict in-plume concentrations for plumes narrower than the inner grid-cell resolution (1 km in this study).

Most PM_{2.5} components were reasonably well modelled in the November case study except for organic matter. The more significant over-prediction in organic matter in November by the CCAM modelling was traced to long-range transport of bushfire smoke from north-west Australia. It appears likely that the model over-predicted the generation of secondary organic aerosol in this plume due to high peak temperatures predicted by CCAM. The higher sea-salt aerosol in November has been predicted well by the model, when the predominant wind direction is onshore.

The modelled spatial distributions showed that the four study sites generally covered the range of modelled PM_{2.5} and PM_{2.5} component concentrations except for some localised sources of elemental carbon and organic matter. The model results demonstrate the importance of the continental scale transport of sea salt in determining inland background concentrations in winter.

The measured PM_{2.5} component information from the LHPCS is very useful for the purpose of refining and validating chemical transport modelling. This modelling in turn has enabled the projection of spatial trends in PM_{2.5} component concentrations across the Lower Hunter region, and the projection of PM_{2.5} component concentrations at sites for which measurements were not undertaken, as illustrated for Maitland and Toronto.

References

- Andreae, MO, and Merlet, P: Emission of trace gases and aerosols from biomass burning, *Global Biogeochem Cy*, 15, 955–966, Doi 10.1029/2000gb001382, 2001.
- Azzi, M, Cope, M, and Rae, M: Sustainable Energy Deployment within the Greater Metropolitan Region. NSW- Environmental Trust 2012.
- Azzi, M, Angove, D, Campbell, I, Cope, M, Emmerson, K, Feron, P, Patterson, M, Tibbett, A, and White, S: Assessing atmospheric emissions from an amine based CO₂ PCC process and their impacts on the environment – a case study. Volume 2. Atmospheric chemistry of MEA and 3D air quality modelling of emissions from the Loy Yang PCC plant. CSIRO, Australia, 2013.
- Carslaw, D C, and Ropkins, K: openair – An R package for air quality data analysis, *Environ Modell Softw*, 27-28, 52-61, 10.1016/j.envsoft.2011.09.008, 2012.
- Clarke, A, Kapustin, V, Howell, S, Moore, K, Lienert, B, Masonis, S, Anderson, T, and Covert, D: Sea-salt size distributions from breaking waves: Implications for marine aerosol production and optical extinction measurements during SEAS, *J Atmos Ocean Tech*, 20, 1362–1374, 2003.
- Cope, M, Keywood, M, Emmerson, K, Galbally, I, Boast, K, Chambers, S, Cheng, M, Crumeyrolle, S, Dunne, E, Fedele, F, Gillett, RW, Griffiths, A, Harnwell, J, Katzfey, J, Hess, D, Lawson, S, Miljevic, B, Molloy, S, Powell, J, Reisen, F, Ristovski, Z, Selleck, P, Ward, J, Zhang, C, and Seng, J: The Sydney Particle Study. CSIRO, Australia. Available at <http://www.environment.nsw.gov.au/aqms/sydparticlestudy.htm>, 2014.
- Cope, ME, Hess, GD, Lee, S, Tory, K, Azzi, M, Carras, J, Lilley, W, Manins, PC, Nelson, P, Ng, L, Puri, K, Wong, N, Walsh, S, and Young, M: The Australian Air Quality Forecasting System. Part I: Project description and early outcomes, *J Appl Meteorol*, 43, 649–662, Doi 10.1175/2093.1, 2004.
- Donahue, NM, Robinson, AL, Stanier, CO, and Pandis, SN: Coupled partitioning, dilution, and chemical aging of semivolatile organics, *Environ Sci Technol*, 40, 2635–2643, DOI 10.1021/es052297c, 2006.
- Emmerson, KM: The Air Quality Model Ensemble Project, The Centre for Australian Weather and Climate Research, Australia, 2014.
- Emmerson, KM, Cope, ME, Lee, S, Hibberd, MF, and Torre, P: Modelling atmospheric mercury from power stations in the Latrobe Valley, Victoria, *Air quality and climate change*, 49, 33–37, 2015.
- Fountoukis, C, and Nenes, A: ISORROPIA II: a computationally efficient thermodynamic equilibrium model for K⁺-Ca²⁺-Mg²⁺-NH₄⁽⁺⁾-Na⁺-SO₄²⁻-NO₃⁻-Cl⁻-H₂O aerosols, *Atmos Chem Phys*, 7, 4639–4659, 2007.
- Gong, SL: A parameterization of sea-salt aerosol source function for sub- and super-micron particles, *Global Biogeochem Cy*, 17, 10.1029/2003gb002079, 2003.
- Hibberd, MF, Keywood, MD, Selleck, PW, Cohen, DD, Stelcer, E, Scorgie, Y, and Chang, L: Lower Hunter Particle Characterisation Study. Final report. New South Wales Office of Environment and Heritage, Australia, 2016.
- Lu, H, and Shao, YP: A new model for dust emission by saltation bombardment, *J Geophys Res-Atmos*, 104, 16827–16841, Doi 10.1029/1999jd900169, 1999.

McGregor, JL, and Dix, MR: An updated description of the Conformal-Cubic atmospheric model, *High Resolution Numerical Modelling of the Atmosphere and Ocean*, 51–75, Doi 10.1007/978-0-387-49791-4_4, 2008.

Sarwar, G, Luecken, D, Yarwood, G, Whitten, GZ, and Carter, WPL: Impact of an updated carbon bond mechanism on predictions from the CMAQ modeling system: Preliminary assessment, *J Appl Meteorol Clim*, 47, 3–14, Doi 10.1175/2007jamc1393.1, 2008.

Sarwar, G, Appel, KW, Carlton, AG, Mathur, R, Schere, K, Zhang, R, and Majeed, MA: Impact of a new condensed toluene mechanism on air quality model predictions in the US, *Geosci Model Dev*, 4, 183–193, DOI 10.5194/gmd-4-183-2011, 2011.

Seinfeld, JH, and Pandis, SN: *Atmospheric chemistry and physics: from air pollution to climate change*, Wiley, New York, xxvii, 1326 p. pp., 1998.

Tsimpidi, AP, Karydis, VA, Zavala, M, Lei, W, Molina, L, Ulbrich, IM, Jimenez, JL, and Pandis, SN: Evaluation of the volatility basis-set approach for the simulation of organic aerosol formation in the Mexico City metropolitan area, *Atmos Chem Phys*, 10, 525–546, 2010.

Walters, DN, Best, MJ, Bushell, AC, Copsey, D, Edwards, JM, Falloon, PD, Harris, CM, Lock, AP, Manners, JC, Morcrette, CJ, Roberts, MJ, Stratton, RA, Webster, S, Wilkinson, JM, Willett, MR, Boutle, IA, Earnshaw, PD, Hill, PG, MacLachlan, C, Martin, GM, Moufouma-Okia, W, Palmer, MD, Petch, JC, Rooney, GG, Scaife, AA, and Williams, KD: The Met Office Unified Model Global Atmosphere 3.0/3.1 and JULES Global Land 3.0/3.1 configurations, *Geosci Model Dev*, 4, 919–941, 10.5194/gmd-4-919-2011, 2011.